DNA 5685F-3

DEFENSE SUPPRESSION

LEVEL II

12

Volume III – Appendix B:

Air Defense Assessment Model (ADAM)

D. A. Cohen
B. A. Falkner
T. A. Pucik
R. K. Siskind

R&D Associates
P.O. Box 9695
Marina del Rey, California 90291

1 May 1979

Final Report for Period 1 May 1978—1 May 1979

CONTRACT No. DNA 001-78-C-0276

APPROVED FOR PUBLIC RELEASE;
DISTRIBUTION UNLIMITED.

THIS WORK SPONSORED BY THE DEFENSE NUCLEAR AGENCY
UNDER RDT&E RMSS CODE B325078464 V99QAXNI06210 H2590D.

Prepared for
Director
DEFENSE NUCLEAR AGENCY
Washington, D. C. 20305

125

Destroy this report when it is no longer needed. Do not return to sender.

PLEASE NOTIFY THE DEFENSE NUCLEAR AGENCY, ATTN: STTI, WASHINGTON, D.C. 20305, IF YOUR ADDRESS IS INCORRECT, IF YOU WISH TO BE DELETED FROM THE DISTRIBUTION LIST, OR IF THE ADDRESSEE IS NO LONGER EMPLOYED BY YOUR ORGANIZATION.

DNA PRINTING PLANT

UNCLASSIFIED

SECURITY CLASSIFICATION OF THIS PAGE (When Data Entered)

REPORT DOCUMENTATION PAGE		READ INSTRUCTIONS BEFORE COMPLETING FORM
1 REPORT NUMBER DNA 5685F-3	2 GOVT ACCESSION NO. AD-A10971	3. RECIPIENT'S CATALOG NUMBER
4. TITLE (and Subtitle) DEFENSE SUPPRESSION Volume III—Appendix B: Air Defense Assessment Model (ADAM)		5 TYPE OF REPORT & PERIOD COVERED Final Report for Period 1 May 78—1 May 79 6 PERFORMING ORG REPORT NUMBER R&D 08902-003
7 AUTHOR(s) D. A. Cohen B. A. Falkner T. A. Pucik R. K. Siskind		8 CONTRACT OR GRANT NUMBER(s) DNA 001-78-C-0276
9 PERFORMING ORGANIZATION NAME AND ADDRESS R & D Associates P.O. Box 9695 Marina del Rey, California 90291		10 PROGRAM ELEMENT, PROJECT, TASK AREA & WORK UNIT NUMBERS Subtask V99QAXNI062-10
11. CONTROLLING OFFICE NAME AND ADDRESS Director Defense Nuclear Agency Washington, D.C. 20305		12 REPORT DATE 1 May 1979 13 NUMBER OF PAGES 70
14. MONITORING AGENCY NAME & ADDRESS(if different from Controlling Office)		15 SECURITY CLASS (of this report) UNCLASSIFIED 15a. DECLASSIFICATION DOWNGRADING SCHEDULE

16. DISTRIBUTION STATEMENT (of this Report)

Approved for public release; distribution unlimited.

17 DISTRIBUTION STATEMENT (of the abstract entered in Block 20, if different from Report)

18 SUPPLEMENTARY NOTES

This work sponsored by the Defense Nuclear Agency under RDT&E RMSS Code B325078464 V99QAXNI06210 H2590D.

19. KEY WORDS (Continue on reverse side if necessary and identify by block number)

Air Defense Model
Simulation
Attrition Model
Many-On-Many
Close Air Support
Battlefield Interdiction
Intervisibility

20 ABSTRACT (Continue on reverse side if necessary and identify by block number)

Appendix B describes RDA's Air Defense Assessment Model (ADAM) which was used in the study to determine a baseline attrition rate for close air support and battlefield interdiction missions and to estimate the effects of ground-based jamming on this attrition rate. Parameters used in the model are defined and their roles are discussed. (Specific values of the parameters for Soviet systems may be found in Appendix A.) The model's

DD FORM 1 JAN 73 1473 EDITION OF 1 NOV 65 IS OBSOLETE

UNCLASSIFIED

SECURITY CLASSIFICATION OF THIS PAGE (When Data Entered)

20. ABSTRACT (Continued)

/unique treatment of line-of-site visibility as affected by typical terrain in the region of interest is described in detail.

TABLE OF CONTENTS

LIST OF ILLUSTRATIONS

SECTION B-1. OVERVIEW OF MODEL

B-1.1 INTRODUCTION

The Air Defense Assessment Model (ADAM), developed at R & D Associates, measures the amount of attrition that a group of aircraft might expect to suffer when flying a designated flight profile through enemy ground-based air defenses. The model handles defense sites, penetrating aircraft, and missile-aircraft engagements on an individual basis rather than aggregating the encounters as is done in some simpler models. ADAM uses Monte Carlo techniques to determine:

- The visibility of a given aircraft relative to a given defense site.
- The time from initial detection opportunity to acquisition by a defense site.
- The outcome of a specific engagement between a missile or antiaircraft gun and an aircraft.
- The status (operable or inoperable) of each defense site.

Hence, several repetitions of any one run are required to average out statistical fluctuations in the results.

ADAM might be regarded as occupying a "middle-of-the-road" position in the spectrum of air defense attrition models. It has more detail than the aggregated models which are often used to estimate the probability of survival for

a specified mission, but it does not begin to approach the complexity of a large-scale model such as TACOS. ADAM is limited to the examination of attrition due to ground-based defenses. It cannot handle air-to-air combat or the effect of aircraft attrition upon other aspects of overall force effectiveness. It is limited at present to handling one wave of aircraft at a time and cannot satisfactorily measure the interaction between simultaneous attacks along different routes or attacks spaced in time along the same route. It can handle the effects of defense suppression techniques and aircraft maneuvers only indirectly by variation of the input parameters. These deficiencies, which are discussed further in later sections, can be balanced against the advantages of relatively fast run times, straightforward inputs, and individually treated engagements. The results from ADAM, while they may not faithfully represent the results of an actual combat situation, can be expected to reflect relative differences in attrition arising from different flight profiles, defense deployments or defense capabilities. An understanding of the assumptions, capabilities, and limitations of ADAM is essential for anyone wishing to use the model or interpret its output. The discussion which follows describes ADAM in sufficient detail for this purpose, but is not concerned with such specifics as input or output format.

B-1.2 MODEL INPUT

Input to ADAM may be subdivided into three main classes:

1. Weapon system characteristics and capabilities.
2. Defense deployments.
3. Aircraft flight profiles.

and a fourth "catch-all" category containing miscellaneous inputs.

B-1.2.1 Weapon System Characteristics

For each weapon type of interest, those characteristics essential to determining when engagement of an aircraft is possible and what the probabilistic outcome of a given engagement will be, must be specified as input. Intercept range and altitude limitations, missile fly-out parameters, various delay times, unit availability, weapon system reliability and kill probabilities are among the variables to which values must be assigned. A complete listing of the weapon system parameters and a discussion of the meaning of each can be found in Section B-3 of this appendix.

For the defense suppression analysis in Section 3 of the main body of this report, the weapon systems of interest were the SA-4, SA-6, SA-7, SA-8, SA-9, ZSU-23-4, and, in a modified sense, the Long Track early-warning/acquisition radar. Input data for these systems, as used in the analysis, are classified and are provided in Appendix A: Soviet Ground-Based Air Defenses.

The weapon system characteristics form a relatively constant set of input. Once assembled, data in this category need only be varied when it is desired to run an excursion requiring modification of intercept range, site availability, kill probability, etc. The modeling of defense suppression techniques may occasion such modifications.

B-1.2.2 Defense Deployments

The air defense sites are located on a rectangular grid. Each site is specified by its x and y coordinates and identified as to weapon type. The appropriate weapon system parameters introduced in Subsection B-1.2.1 thus become associated with the individual sites. Furthermore, each site is classified as to the nature of the surrounding terrain and the quality of the site. For the scenario of interest, set in the Fulda Gap area of West Germany, the terrain is generally characterized as hilly for all defense sites.

Each site is also specified as "preplanned," "expedient" or "immediate" in an attempt to represent the effect of movement rate on site selection and quality. Terrain type and site type are used in ADAM to select the appropriate set of intervisibility statistics as described more fully in Section B-2. ADAM's treatment of intervisibility (or the existence of an unobscured line of sight between defense site and target aircraft) is one of the model's unique features. It utilizes the essential information from site data without loading digitized terrain data into the computer.

B-1.2.3 Aircraft Flight Profiles

Attacking aircraft are assumed to attack in waves. The members of a wave fly a parallel formation and are evenly spaced along a line perpendicular to the direction of the path. The desired penetration path is approximated by a finite collection of line segments joined to each other at node points where profile characteristics are specified. Aircraft altitude, aircraft velocity and total corridor

width are specified at each node along the path. Velocity and interaircraft spacing may change instantaneously at a node as may the direction of the path. When different altitudes are given at adjoining nodes, the model interpolates linearly along the connecting segment to determine values for altitude-related parameters such as intervisibility probabilities, intercept ranges and kill probabilities.

Figure B-1 illustrates the sudden changes in direction and position which can occur at a node point. The basic flight path connecting points A, B, and C is provided by the user as is the number of aircraft (5), and the corridor width (W_1 on segment AB and W_2 on segment BC). At the node point B where the path changes direction, all aircraft except the one which follows the basic flight path instantaneously shift position as well as direction. Though unrealistic, these shifts are regarded as compensating in that some aircraft will be moved closer and some farther from a fixed defense site.

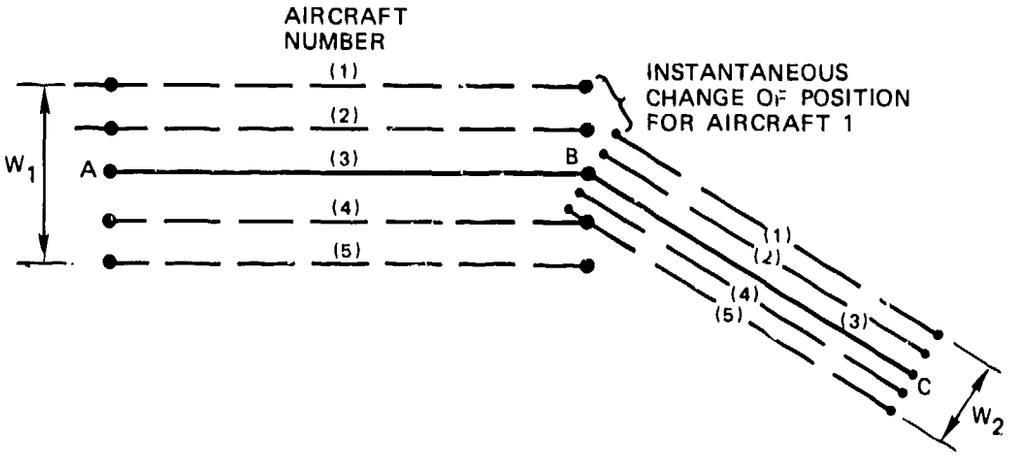

Figure B-1. Nodal Changes in Direction and Position

B-1.2.4 Miscellaneous Input

Ammunition Resupply Doctrine: Successive waves along the same path or differing paths are handled independently by ADAM. However, the effect of the time interval between attack waves on the air defense weapon systems may be approximated by choosing whether or not to resupply the weapon systems to their original level.

Simultaneous Engagement Limit: The user may limit the number of defense weapon sites that may simultaneously engage any one target. A limit of four has been used in most past simulations. This limit seems to have negligible effect on runs involving several aircraft and typical defenses; it would be significant in the case of one or two aircraft flying into heavily defended areas.

Game Time-Step Interval: ADAM is an event-oriented model which examines the aircraft-air defense interaction at fixed moments in time to update its catalog of ongoing events. The time interval between successive looks is a model input usually taken as one second.

Intervisibility Correlation Factor: The user may determine whether or not the individual flight paths in a wave should be simultaneously visible relative to a given defense site. Alternatively, the intervisibility patterns may be generated independently for aircraft in a wave. The second alternative, though not realistic for closely spaced aircraft, probably reduces run-to-run variability.

Output Format Options: There are several options available as to the form of printed output. They vary primarily in the degree of detail provided and will not be discussed further.

Site Intervisibility Statistics Type: The intervisibility statistics may be regarded as input, but are really an inherent part of the model. Statistics have been determined for two terrain types, three site types and four aircraft altitudes. Section B-2 is devoted to a discussion of how these statistics were generated and how they are used in the model.

B-1.3 GENERAL SEQUENCE OF EVENTS

At each node point, the x and y coordinates of defense sites and aircraft positions are rotated and translated as necessary in the program so that the paths proceed parallel to each other in the direction of the positive x axis. A time increment, Δt, therefore generates an increment in aircraft position along the path of $\Delta X = V \cdot \Delta t$ where v is the aircraft velocity. The user specifies the time increment; the associated position increment will take different values on different path segments if aircraft velocity varies.

The model first examines the interplay between defense sites and aircraft at the flight path origin. It then proceeds by stepping along the flight path in increments determined by the time increment, Δt, looking at each step for new engagement opportunities, kill possibilities, and other events.

At each new value of x the model identifies those sites which on the basis of their x coordinate, availability, engagement status and intercept envelope (maximum range, maximum and minimum altitude) would be candidates to initiate an engagement sequence against one or more tracks in the wave.

Tracks are then tested individually against these sites to determine if an engagement is actually possible. Requirements for the initiation of an engagement sequence include:

1. Fire unit availability--the site must have a fire unit which is not currently engaging a target.

2. Track availability--the track must be currently engaged by less than the maximum number of sites.

3. Visibility--the track must be visible to the site.

4. Altitude--the track altitude must be between the minimum and maximum effective altitudes of the site.

5. Engagement area--the target must be within certain bounds determined by the maximum detection range, scan time and maximum effective intercept range of the site which make it likely that an intercept point within the intercept envelope can be computed. This restriction is imposed to cut down on intercept calculations which would probably lead to intercept points beyond the intercept envelope.

6. Continued visibility--the track must remain visible (with the exception of intervals less than the

system's "breaklock" time) until the target is acquired and the appropriate delays prior to launch are enacted. Visibility must also be maintained after launch for a user-specified "look ahead" time (which may be zero).

7. Intercept point--after the appropriate delay times are considered, the missile launch time, missile flyout parameters, guidance type, aircraft offset from the site and aircraft velocity are used to determine the intercept point. (This is a two-dimensional computation in ADAM.) The intercept point must fall within the bounds of the site's intercept envelope.

The determination of whether an engagement can be initiated requires that the model look beyond the current moment to the ensuing intervisibility between the individual site and individual target. The visible/masked pattern is generated from the intervisibility statistics by means of Monte Carlo (or random number) techniques. ADAM looks ahead to the launch time (and in some cases a few seconds beyond launch time) to determine whether or not visibility permits a launch to take place. It looks still further in the case of command-guided or semiactive homing missiles, to the computed intercept point to determine if an intercept with its associated target kill opportunity can really take place. A breaklock during this interval will not deter an engagement by the site but will prevent the intercept from taking place. It will also affect the time at which the fire unit will be released from the engagement to seek new targets.

In summary, when dealing with an individual target and a weapon site which passes all of the tests for engagement, ADAM can look ahead to determine:

- Launch time.
- Intercept time.
- Breaklocks that will prevent intercept.
- Engagement kill probability, P_K, based on the number of weapons salvoed, the intercept range, the weapon system reliability, the target altitude and the weapon SSPK.
- Expected weapon system release time.

A gun system or IR system such as the SA-7 or SA-9 would normally be released from an engagement at the moment of final weapon launch. Other missile systems considered, such as the SA-4, SA-6, or SA-8, require that the fire unit remain involved with an engagement until the projected intercept time or until a breaklock occurs.

Interactions with other weapons engaging the same target may, however, cause unforeseen changes in the event sequence computed for a given weapon site. For example, a second weapon site might engage a target and kill it prior to the first weapon's launch time or during its flight time. In the first case, the original site would not fire; in either case, the original site and any other site engaging the target would be immediately released.

Thus, rather than taking actions based on future events, ADAM records the launch time, intercept time or breaklock time, expected release time, number of shots fired and the computed P_K for an engagement. When more than one fire unit engages the same target, the model keeps track of this information for all engaging units and specifically singles out the next occurring intercept time or kill opportunity. As the model progresses stepwise along the path of the wave, it examines each track and makes appropriate changes in the number of weapons remaining and the engagement status of the sites engaging it. Whenever a kill opportunity occurs, it performs a random draw against the P_K to determine the fate of the aircraft and to classify the missiles involved as kills or misses. If a kill occurs, other engaging weapon systems are released and their missiles, if fired, are counted as wastes.

Even if no engagement is initiated because of visibility problems or other causes, the random seed used to generate the visibility pattern for the given site/track combination is stored so that subsequent attempts by the site to engage the track will be subject to the same masking effects.

Aside from its intervisibility procedures, ADAM works essentially as a bookkeeper keeping track of a vast amount of interacting information. It organizes and prints the input data to the detail desired. It maintains a continuous record of the shots fired by each individual site and by sites of a given type; the shots are classified as misses, kills and wastes. For each aircraft track, it records when the track is killed as well as the number of shots expended on the track. It keeps statistics on the overall attrition rate. Results of the battle are then printed to the detail specified by the user.

SECTION B-2. INTERVISIBILITY

B-2.1 INTRODUCTION

The ADAM model is capable of "flying" large numbers of aircraft over large defensive arrays to investigate aircraft attrition and its dependence on aircraft speed and altitude, as well as on individual air defense system characteristics. Since ground-to-air visibility is viewed as an important factor in such analyses, a quantitative characterization of visibility was needed for incorporation into the design of ADAM. This could have been achieved by using digitized terrain data directly to analyze the intervisibility of each site location. However, in view of the large amount of data required, it was felt that this would be unduly cumbersome and time-consuming, that it would impair the flexibility of the model, and that the results might be overly specific to the particular choice of defense placements and aircraft flight paths. For these reasons, an alternative approach was adopted in which ground-to-air visibility was quantified statistically as a function of site quality and aircraft altitude.

Key indicators of aircraft vulnerability are the length, range and spacing of those intermittent segments of the traverse for which the aircraft is visible to the site. The model must be able to generate these intervals. In conjunction with a specified aircraft ground speed, these "exposure lengths" can be converted into exposure times and compared to the acquisition and fly-out times for a given air defense system to determine whether a firing opportunity occurs. Conversely, brief interruptions in the visible segments can be translated into interruption times and

compared to the breaklock time of the air defense system to determine whether they are sufficient to delay or nullify an engagement opportunity.

B-2.2 SITE SELECTION

In order to collect statistical information on these exposure lengths, intervisibility analyses were first conducted for selected site locations in the Fulda area. The terrain in this region of West Germany is hilly and mountainous with close to one-half the area covered by forests. The area contains many valleys that are dominated by a complex array of hilly ridgelines. Many of the valleys are interconnected and form natural corridors through the region. The terrain elevations range from less than 200 m in the lowest valleys to between 450 to 600 m in the hills and mountains, although some of the more prominent peaks exceed 750 m.

The variation of the terrain in this region makes the amount of time the air defense systems have to select deployment sites a critical factor in determining the quality of the air defense coverage. Most of the roads in this region follow the natural corridors formed by the many valleys, so that the most accessible deployment sites are located within these valleys. These deployment sites, although readily available, are less desirable because of the high degree of local masking. The optimum deployment sites, in terms of visibility, are located atop the higher hills, away from the roads, in the more inaccessible regions. Given enough time, most of the air defense systems would deploy to these optimum sites for the increased visibility. However, in a mobile environment where the air defenses will have to

move often or deploy rapidly, the time available for site access may be short. The effect will be that the air defense systems will be forced to deploy at less than optimum sites with the resulting degradation in visibility.

Three classes of deployment sites were selected to represent the influence that environment mobility will have on the quality of the air defense coverage. The amount of deployment time was used to exemplify the degree of mobility and categorize the site type. All of the sites selected were accessible by cross-country travel from a road and positioned, when possible, in clearings free of trees. The three classes of sites selected were:

1. Preplanned. A preplanned site corresponds to a static environment in which the air defenses could have an indefinite amount of time to select a deployment site. These sites are generally located on top of the higher hills so as to be above the many ridges and peaks in the region.

2. Expedient. An expedient site corresponds to a slow to moderate movement environment in which the air defense systems will have to move on a regular basis to maintain adequate coverage. The expedient sites were selected to be within thirty minutes travel time or five kilometers from the road. These sites are generally located on locally high hills that provide as much visibility of the road and surrounding area as possible.

3. Immediate. An immediate site corresponds to a rapid movement environment in which the air defense systems

will have to move directly with the supported units to keep pace. The sites were selected to be within five minutes travel time or one kilometer from a road.

A total of thirty deployment sites, ten per site class, were selected for analysis.

B-2.3 TERRAIN DATA BASE

The analysis was based upon a series of digitized terrain data tapes produced by the Defense Mapping Agency Topographic Center. The fifteen data tapes in the series contained the UTM coordinates and the associated elevation of the terrain for over 60 million terrain points in a 9000-square kilometer region centered about the town of Fulda, West Germany. The excessively large number of data points required an expansion in grid size from the original spacing of 12.5 m to 50 m and a corresponding 16-fold reduction in number of data points. The elevations stored on the data tapes represented only the surface elevation of the terrain in this region. The location and elevation of other features such as trees and towns were not included on the tapes. As a result, the influence these obstructions would have on the ground-to-air visibility was not considered in the initial computations. (A preliminary analysis made to estimate the effects of trees on the line-of-site indicated that visibility may be further reduced, sometimes by appreciable amounts.)

With these data, it was possible to "fly" aircraft past selected site locations and determine where they would be visible and where they would be masked, as illustrated

schematically in Figure B-2. For each site, visibility analyses were performed for four terrain-following aircraft altitudes: 38, 75, 150 and 300 m above ground level (AGL).

A typical result of these analyses is the intervisibility map shown in Figure B-3. Conceptually, each horizontal scan in this example can be viewed as a traverse by a terrain-following aircraft flying at 75 m AGL past an observer located at the center of the circle, seen in plan view. Dark segments denote portions of the traverse where the line-of-sight (LOS) between observer and aircraft is obstructed by intervening terrain features; light segments denote portions where the LOS is clear and the aircraft is visible. The pattern of light and dark areas provides some indication as to the relative roughness of this area, as well as the characteristic length of the terrain features. This particular site is situated in a very favorable location, atop a prominent hill, and yet the aircraft derive a considerable benefit by flying in a low-altitude, terrain-following mode. For less well selected site locations, the benefits to the aircraft can be expected to be even greater in this type of terrain.

Intervisibility maps are shown in Figure B-4 for representative preplanned, expedient and immediate sites. The ground-to-air visibility is shown for a radius of 38.5 km around each site. The visibility is for an optical LOS with the radar positioned three meters above the terrain. The dark area represents a region where an aircraft in a perfect terrain-following mode is masked from view of the site and the open area where an aircraft is visible to the site. The intervisible regions are shown for each site at aircraft altitudes of 75, 150 and 300 m AGL.

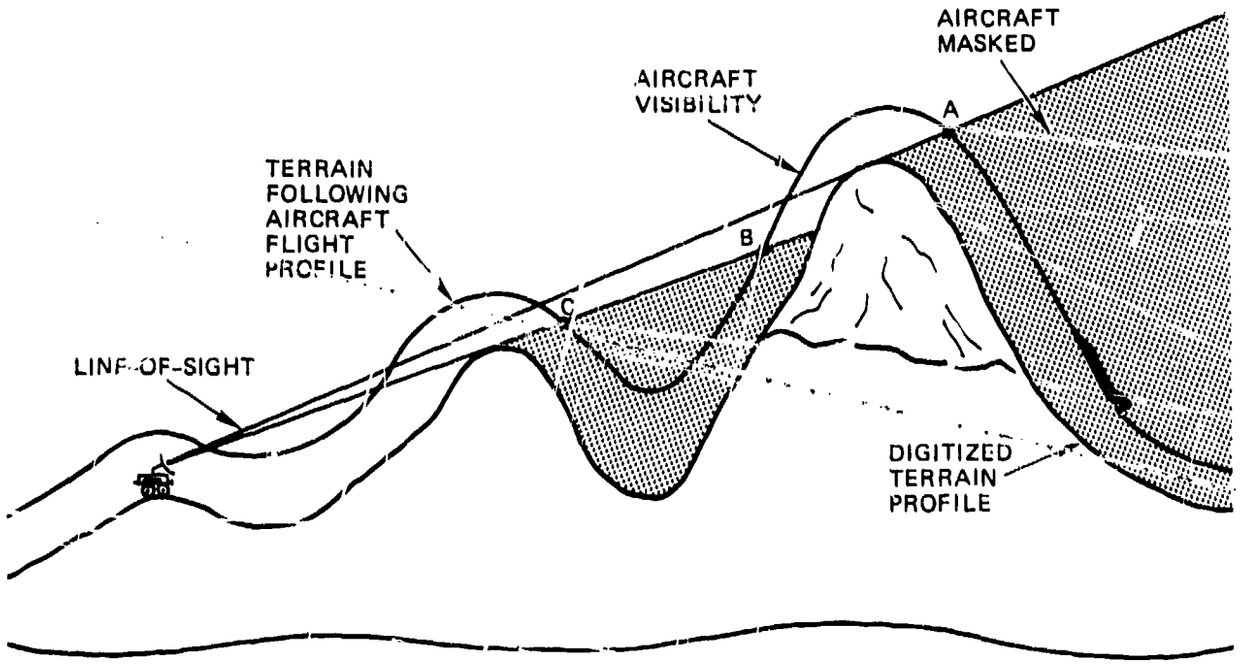

Figure B-2. Intermittent Aircraft Visibility Resulting from Terrain Masking

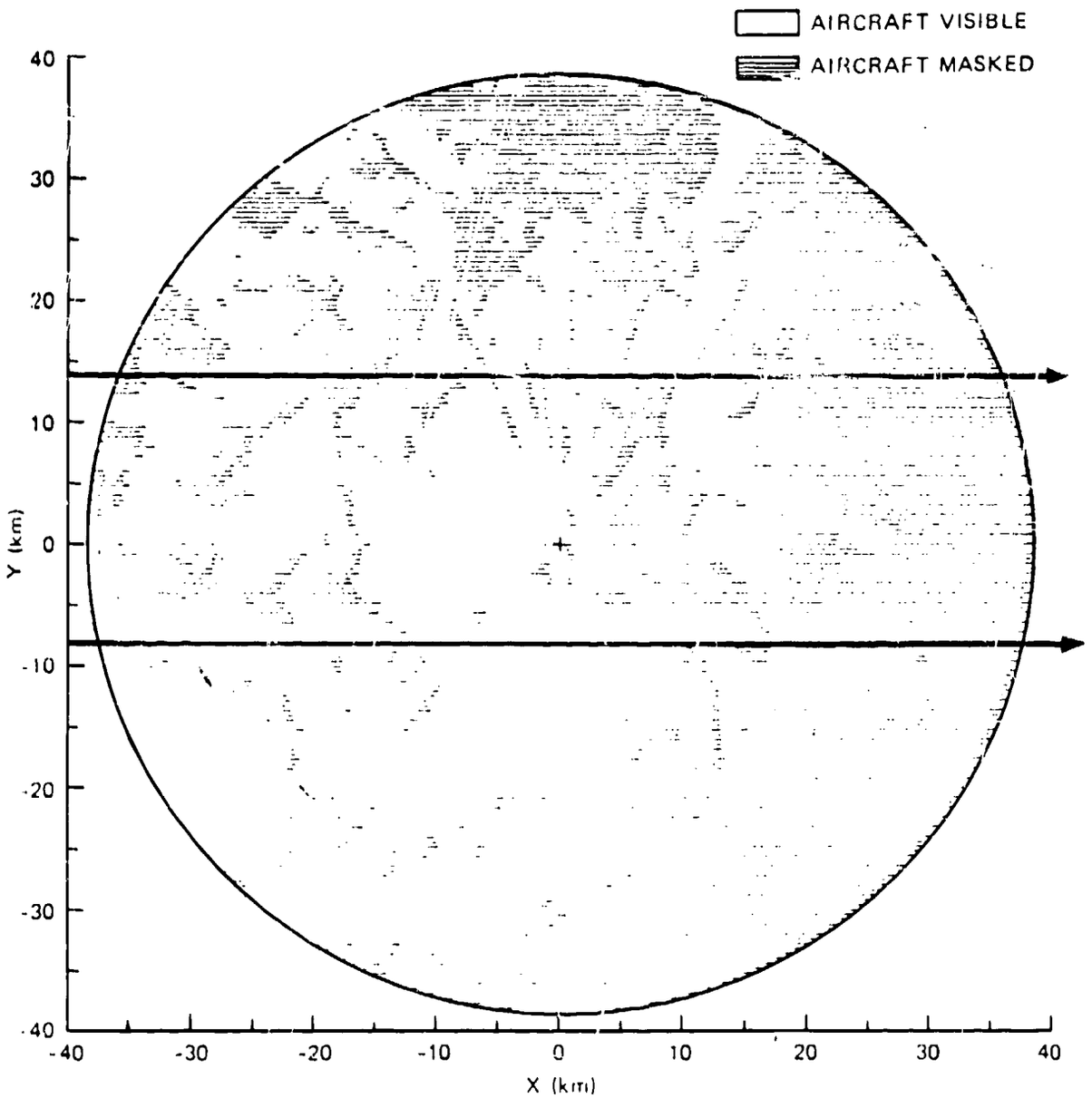

Figure B-3. Intervisibility Map for a Preplanned Site in the Fulda Region; Aircraft Flying in Terrain-Following Mode at 75 m Above Ground Level

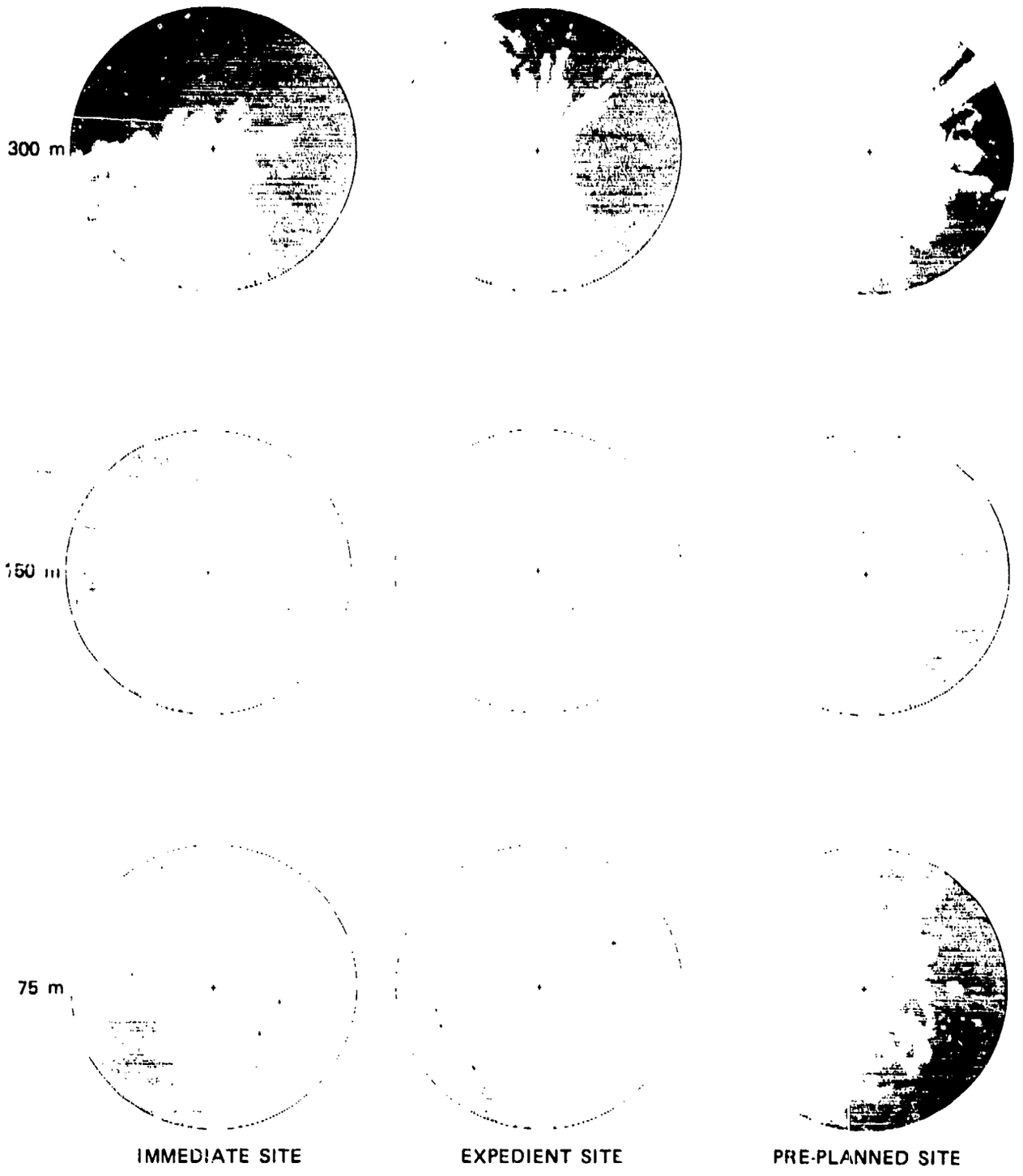

Figure B-4. Intervisibility Map for a Preplanned, Expedient and Immediate Site at Aircraft Altitudes of 75, 150 and 300 m

As is evident, the area of visibility is greatest for the preplanned site and decreases for the expedient and immediate sites. The visibility "opens up" for the preplanned site at altitudes greater than 150 m so that for higher altitudes the visibility is virtually unlimited. The visibility for the expedient and immediate sites just starts to "open up" at 300-m altitude. Even so, an air defense system located at any one of the sites will not be restricted from engaging aircraft at altitudes greater than 300 m because of a lack of visibility.

B-2.4 ANALYSIS - VISIBILITY STATISTICS

The ground-to-air visibility patterns computed for thirty selected sites (10 preplanned, 10 expedient and 10 immediate) and four aircraft altitudes were used as the basis for the statistical intervisibility incorporated into ADAM.

The statistics used in the model must be capable of generating intervals along a flight path where the aircraft is alternately visible and invisible to a given defense site. The lengths, spacings and locations of the visible intervals should resemble, in a probabilistic sense, the patterns derived from digitized terrain data.

Two fundamental parameters underlying the probabilistic visibility model are the "probability of point visibility," P_{pv}, and the "probability of a change in visibility status," P_{cs}. The first parameter is a dimensionless quantity denoting the likelihood that an aircraft will be visible to the site at a randomly selected point along its traverse. The second parameter denotes the likelihood that the aircraft

will undergo a change in visibility state (either from masked to visible or from visible to masked) in a unit increment of travel along the traverse, and has the dimensions of $(\text{length})^{-1}$.

Conceptually, these two parameters can be estimated by performing visibility analyses for large numbers of aircraft traverses past representative site locations. By collecting data on the average fraction of the traverse length for which the aircraft is visible to the site, one obtains an estimate of the probability of point visibility, P_{pv}. Similarly, the probability of a change in visibility status, P_{cs}, can be estimated by summing the total number of observed state changes and dividing by the total traverse length to obtain an average density of changes per unit length of travel.

Both parameters are important in determining the likelihood that an air defense site will have a firing opportunity on a penetrating aircraft. The parameter P_{pv} reflects the likelihood that the aircraft will be visible at a randomly chosen point along its traverse, but provides no indication as to the duration of visibility. (For example, along a 100-km traverse, a visible fraction of 0.5 may correspond to one long visible segment and one long masked segment of 50 km each, or it may correspond to 100 intermittent, alternating segments of one kilometer each.) To represent a firing opportunity, an aircraft must not only become visible but must remain visible sufficiently long for the air defense system to acquire and fire. Consequently, additional information regarding the duration or structure of the visibility is necessary in order to evaluate the likelihood of a firing opportunity occurring.

This information is provided by the parameter P_{cs}, which reflects the frequency of changes in visibility status. However, some care is required in the interpretation and usage of the parameter, since its fundamental meaning is easily misconstrued.

Suppose that an incremental segment, dl, of the aircraft traverse is chosen at random, with no foreknowledge of the visibility states at either the beginning or the end of dl. Then, the product $P_{cs} \cdot dl$ represents the probability that, when the actual beginning and ending states are determined, the outcome will be one in which the two visibility states are opposite (masked-visible or visible-masked). There is a subtle but important distinction between this case and the more usual case in which the initial visibility state is known, and one would like to determine the likelihood that the final visibility state will be different. This latter case entails a foreknowledge of the initial visibility state which is inconsistent with the definition of P_{cs}. In fact, the second case must be divided into two subcases dependent upon the visibility state at the initial point, since the probability of going from visible to masked is not generally the same as the probability of going from masked to visible. This is easily seen by considering a sample aircraft traverse characterized by long visible segments punctuated by short and infrequent masked segments. If the aircraft happens to be visible, its likelihood of becoming masked is rather low, whereas if it is masked, its likelihood of becoming visible is quite high. Two parameters are required; these are termed the "visibility birthrate," λ, and the "visibility deathrate," μ, characterized as follows: (a) if the aircraft is masked at the beginning of dl, then the product $\lambda \cdot dl$ represents the probability that it will be

visible at the end of dl; (b) if the aircraft is visible at the beginning of dl, then the product $\mu \cdot dl$ represents the probability that it will be masked at the end of dl. The general procedure is to obtain values of P_{pv} and P_{cs} from visibility analyses; values for λ and μ are then derived from those of P_{pv} and P_{cs}.

In order to reflect the strong dependence of aircraft visibility on range from the site, the parameters P_{pv} and P_{cs} were allowed to vary as a function of range, R. A dependence upon azimuth, θ, could also have been incorporated, but the additional complication did not appear warranted by the marginal benefits that would be derived. Treating visibility as a function of range alone does introduce a certain degree of "cylindrical smearing" into the results, but nevertheless reflects the dominant influence of position relative to the site center.

The parameters λ and μ can be expressed in terms of P_{pv} and P_{cs} and are hence also functions of the range R. Equations (B-1) and (B-2) below have been derived for $\lambda(R)$ and $\mu(R)$.

$$\lambda(R) = \frac{1}{2}\left[\frac{P_{cs}(R)}{\bar{P}_{pv}(R)} - \frac{d}{ds} \text{Ln } \bar{P}_{pv}(R)\right], \qquad \text{(B-1)}$$

$$\mu(R) = \frac{1}{2}\left[\frac{P_{cs}(R)}{\bar{P}_{pv}(R)} - \frac{d}{ds} \text{Ln } P_{pv}(R)\right]. \qquad \text{(B-2)}$$

where $\bar{P}_{pv}(R) = 1 - P_{pv}(R)$ and d/ds is the derivative with respect to the path.

Approximations to (B-1) and (B-2) that do not involve logarithmic derivatives were used in the model to compute the probability of a change in state from masked to visible and the probability of a change from visible to masked during a given time step.

In general, when the average visibility is good [$P_{pv}(R)$ is close to one] the likelihood of going from masked to visible, $\lambda(R)\Delta R$, is much higher than the likelihood of going from visible to masked, $\mu(R)\Delta R$.

The techniques employed in collecting the visibility statistics were designed to reflect this positional dependence. Digitized terrain data furnished terrain-altitude information at discrete points in a square mesh 50 m on a side. A sample site was placed at one of these mesh points, and an intervisibility analysis was conducted to determine the aircraft visibility state at each of the mesh points throughout the entire 84-km x 110-km rectangular region, assuming perfect terrain-following at a specified altitude above ground level. Conceptually, the mesh was then overlayed with a pattern of concentric circles centered at the site location, with radii $R_n = n\Delta R$ $(n = 1,2,3,...)$ where ΔR was 50 m. This divided the area into annular regions where each region could be associated with the index, n, and the radius, R_n, of its outer boundary. To estimate the probability of point visibility, $P_{pv}(R)$, the mesh points were grouped according to the annular region in which they lay. For each region, n, data were collected on the total number of mesh points, $N_T(n)$, lying within the region, as well as on the number of points, $N_v(n)$, for which the aircraft was visible to the site. An estimate of $P_{pv}(R)$ was then given by the average visible fraction, $F_v(R_m)$, defined by

$$F_V(R_n) = \frac{N_V(n)}{N_T(n)} \qquad n = 1,2,3,... \qquad \text{(B-3)}$$

The probability of a change in visibility status, $P_{cs}(R)$, was estimated in a similar way, except that here the major interest was in the line segments lying between adjacent grid points in the square mesh. Each line segment was assigned to an annular region based on the range at its midpoint. For each annular region, n, data were collected on the total number of mesh line segments, $M_T(n)$, lying within the region, as well as on the number of segments, $M_{cs}(n)$, having opposite visibility states at the two mesh points defining the end points of the segment. An estimate of $P_{cs}(R)$ was then given by the average density of changes in visibility status per unit length, $D_{cs}(R)$, defined by

$$D_{cs}(R_n) = \frac{M_{cs}(n)}{\Delta L \cdot M_T(n)} \qquad n = 1,2,3,... \qquad \text{(B-4)}$$

where ΔL is the length of the mesh line segments, or the mesh size (50 m in this case). As a further refinement, data on changes in visibility status were tallied separately for vertical and horizontal mesh line segments in order to determine if there was any substantial difference between the two, which might indicate a dependence on the direction of the traverse. None was found, and the two sets of data were subsequently combined into one.

In order to quantitatively characterize ground-to-air visibility as a function of site quality and aircraft altitude, similar statistics were needed for each generic site type (preplanned, expedient and immediate) at each of the

four selected aircraft altitudes (38, 75, 150 and 300 m above ground level). Visibility analyses were conducted for the ten sample locations of each generic site type.

For a given site type and terrain-following altitude, the values of $F_v(R_n)$ and $D_{cs}(R_n)$ were averaged over the ten sample locations. The average was weighted according to the contributing sample size. (Sites near the periphery of the region for which digitized terrain data was available had a reduced sample size when R_n exceeded the distance to the boundary of the region.) Additional smoothing was obtained through the use of a "running average" in which the value at R_n was averaged together with the values at the neighboring ranges R_{n+1}, $R_{n+2} \cdots R_{n+m}$. The value of m was taken as 12 for all curves shown in this section, so that the running average extends over an interval of $\pm$600 m about each point.

The results are presented in Figures B-5 through B-7, which illustrate both the average visible fraction, F_v, and the average density of changes in visibility status, D_{cs}, as a function of range for the three originally selected aircraft altitudes and for each site-quality category. The importance of aircraft altitude is evidenced in the steady decrease in fractional visibility with decreasing altitude in all three cases. This is accompanied by a steady increase in the density of changes in visibility status, particularly at the shorter ranges, indicating that the visibility also tends to become more erratic and intermittent. It is interesting to note that at longer ranges, the density of changes tends toward nearly the same limiting value for all three altitudes (although the magnitude of this value varies with site quality). This suggests that at these ranges, the expected number of visible segments is roughly the same at

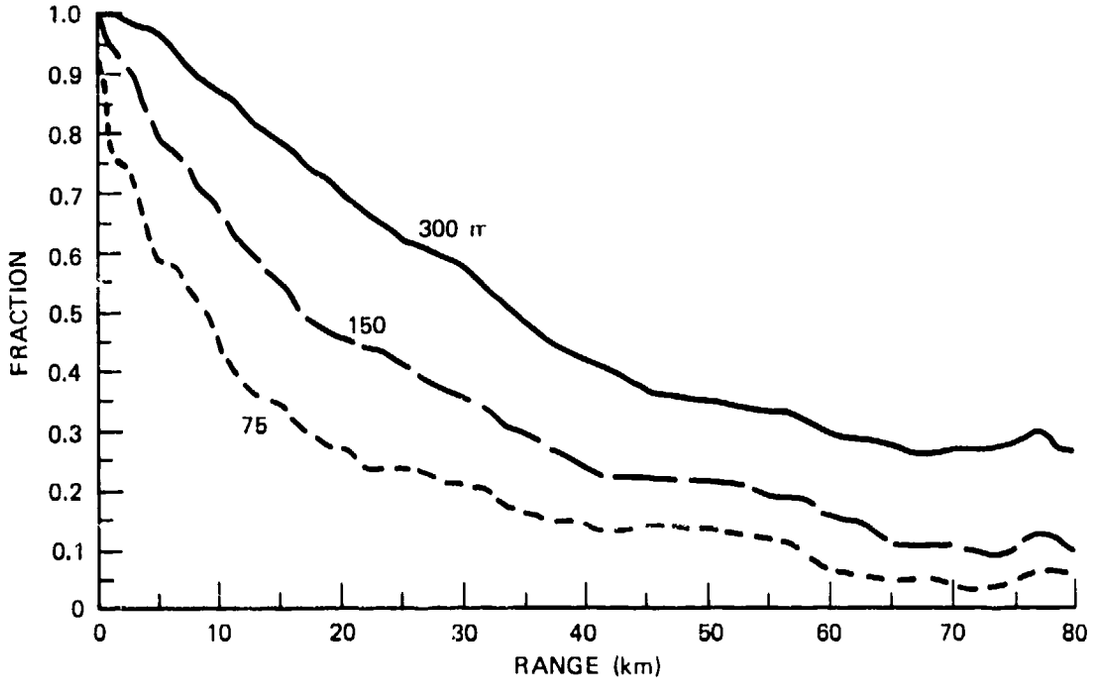

(a) FRACTION OF CIRCUMFERENCE VISIBLE

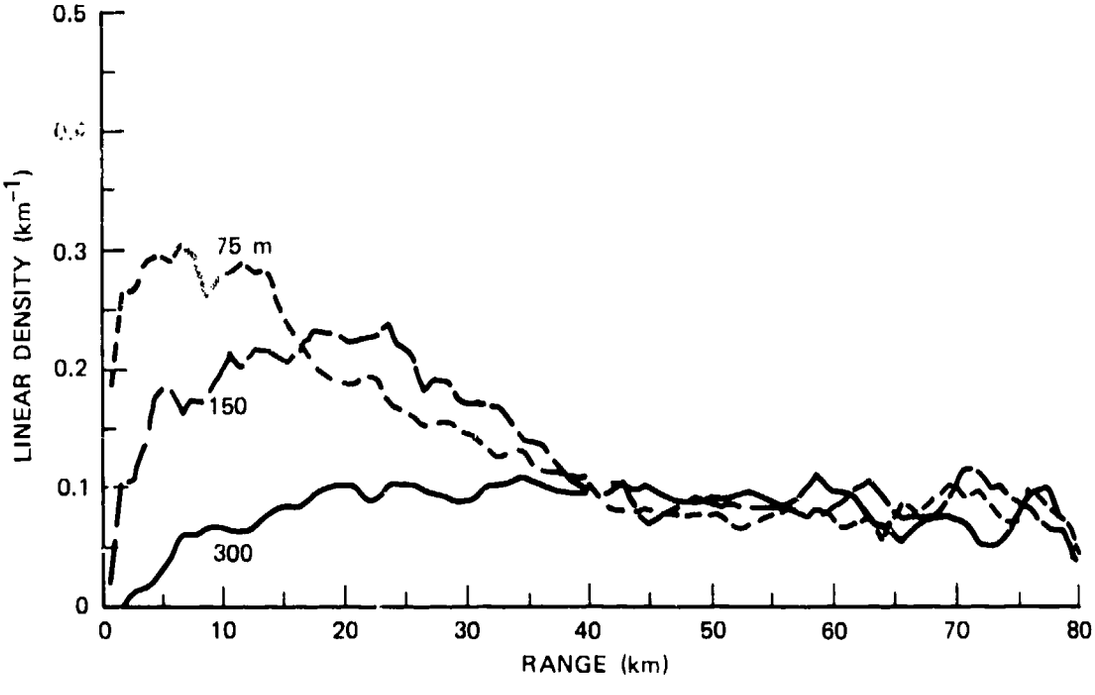

(b) LINEAR DENSITY OF CHANGES IN VISIBILITY STATUS

Figure B-5. Average Visibility Statistics for Preplanned Sites at Aircraft Altitudes of 75, 150 and 300 m Above Ground Level

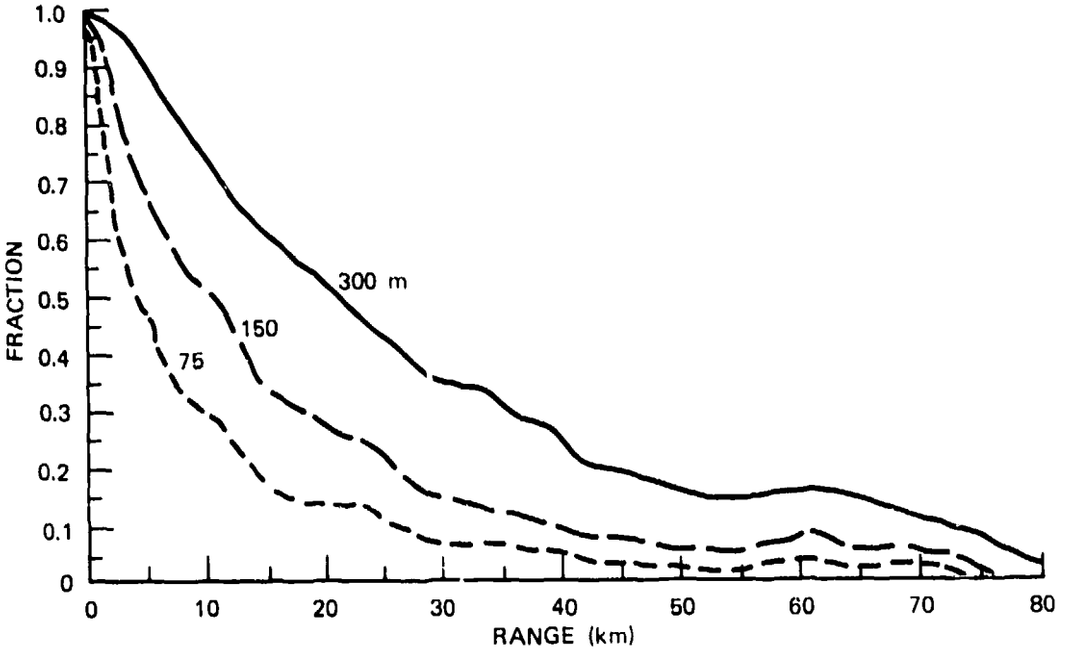

(a) FRACTION OF CIRCUMFERENCE VISIBLE

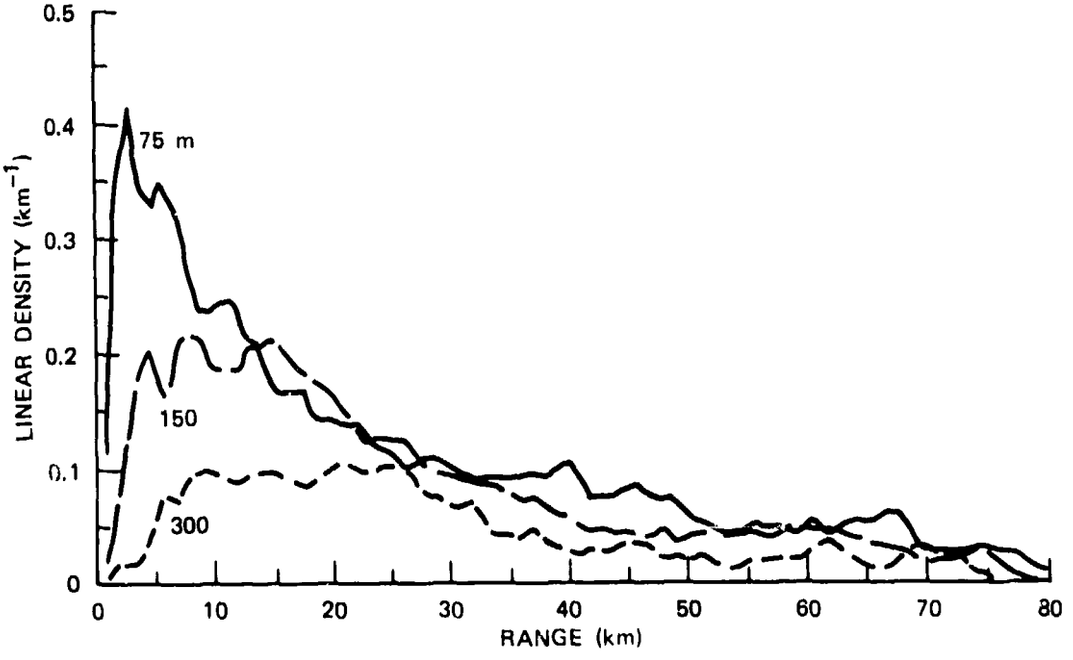

(b) LINEAR DENSITY OF CHANGES IN VISIBILITY STATUS

Figure B-6. Average Visibility Statistics for Expedient Sites at Aircraft Altitudes of 75, 150 and 300 m Above Ground Level

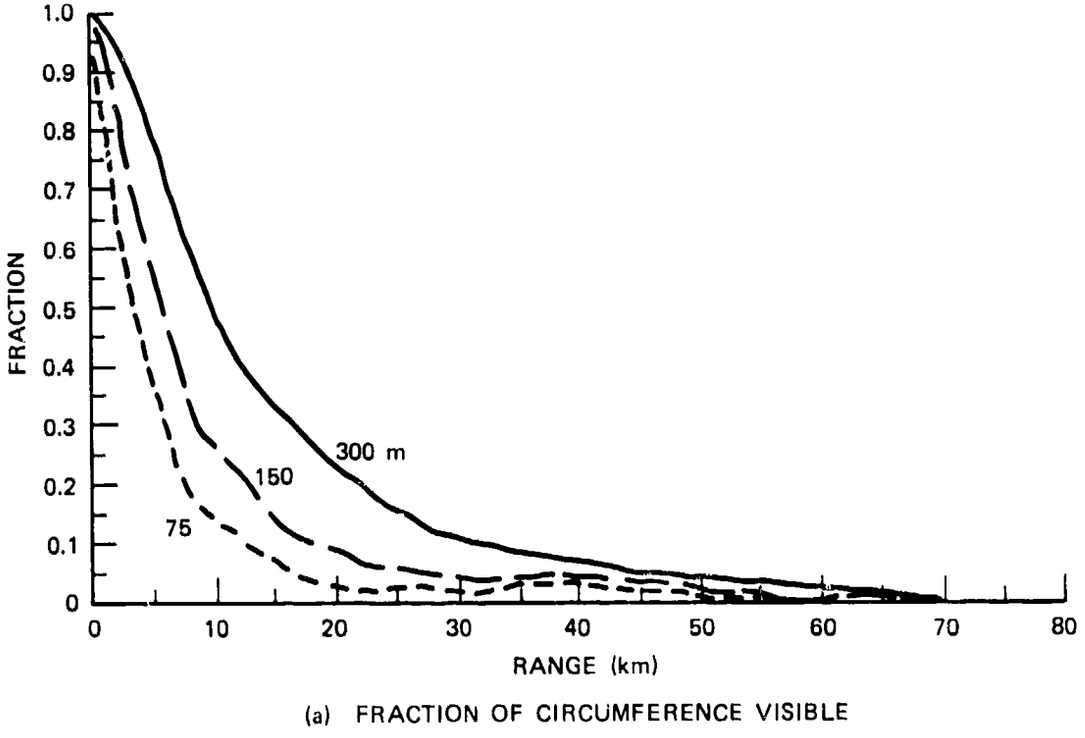

(a) FRACTION OF CIRCUMFERENCE VISIBLE

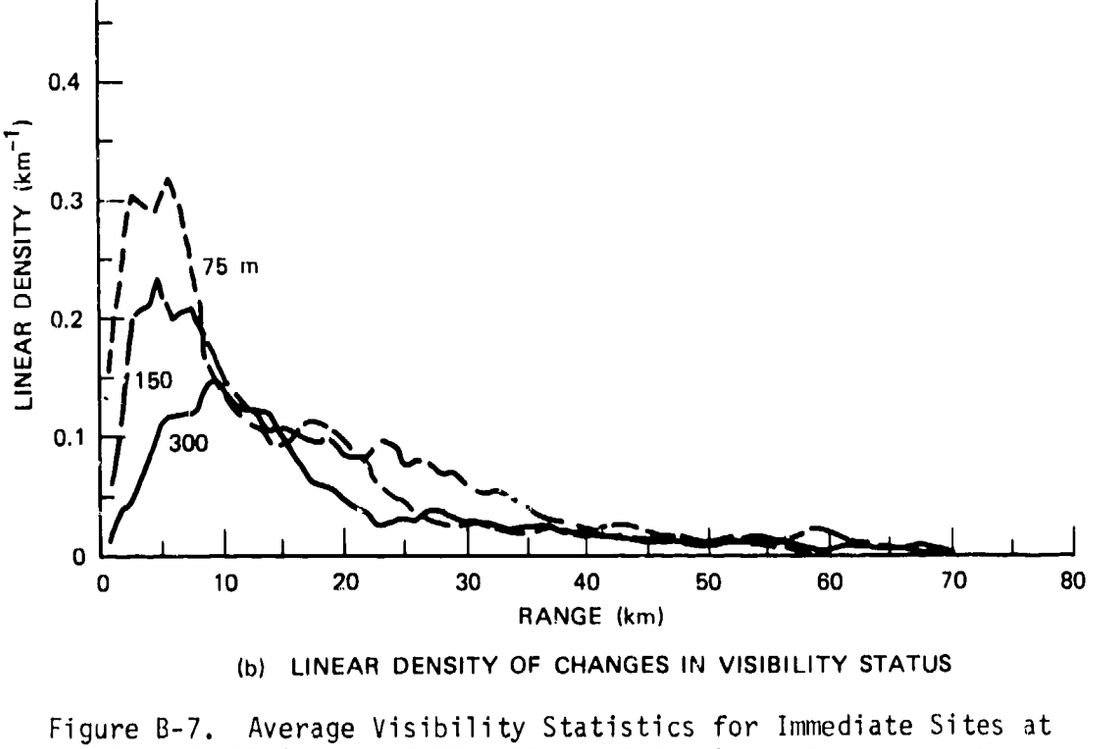

(b) LINEAR DENSITY OF CHANGES IN VISIBILITY STATUS

Figure B-7. Average Visibility Statistics for Immediate Sites at Aircraft Altitudes of 75, 150 and 300 m Above Ground Level

all four altitudes. However, the expected length of each visible segment is lower at the lower altitudes, since the visible fraction is lower. This is consistent with Equations (B-1) and (B-2), which indicate that even if the probabilities of a change in visibility status are roughly comparable at all three altitudes, the lower probabilities of point visibility at the lower altitudes lead to lower visibility birthrates, λ, and to higher visibility deathrates, μ.

The importance of site quality is reflected in the much more rapid dropoff in visible fraction with increasing range for the hastily chosen sites. The preplanned sites are typically located atop the higher hills, and from these vantage points they can generally look across the neighboring hilltops and see aircraft flying above mean hilltop level. As a result, the drop-off in visible fraction is relatively slow particularly at the higher aircraft altitudes. At the other end of the spectrum, the immediate sites tend to be located more in valleys, where surrounding hills and ridgelines may present major obstructions, so that the drop-off is much more rapid for all three aircraft altitudes.

The estimates of the probability of point visibility, $P_{pv}(R)$, and the probability of a change in visibility status per unit length, $P_{cs}(R)$, as given by the graphs in Figures B-5 to B-7 are used within ADAM. They are used to generate representative ground-to-air visibility histories for each aircraft traverse past each site location using Monte Carlo techniques. For incorporation into ADAM, the curves were fitted by seventh-order polynomials. The eight polynomial coefficients for each site type, aircraft altitude and probability function were input into the model so that the functions represented could be reconstructed as needed.

ADAM generates visibility histories in a stepwise fashion along each aircraft track. At each step, the probability of the aircraft being visible to a given site is computed from the visibility coefficients on the basis of aircraft altitude, site type and distance to the site. A random number is then generated and compared to this probability to determine whether the aircraft shall be "visible" or "masked." This outcome, together with the coefficients characterizing the likelihood of the aircraft changing its visibility state in an increment of travel, is then used to compute the probability that the aircraft will be visible at the next step. A second random number is required. The process is repeated until an entire visibility history consisting of alternating periods of visibility and invisibility has been generated.

SECTION B-3. INPUT PARAMETERS FOR SOVIET AIR DEFENSES

B-3.1 INTRODUCTION

This section defines and interprets the air defense system characteristics which are required by ADAM. Most of these inputs are used in the model to determine, in conjunction with the intervisibility history, when a given air defense site can engage a given aircraft. The parameters may be grouped, somewhat imprecisely, into the following classes:

1. Initialization
   - Fire units/site
   - Initial number of shots

2. Defense system availability
   - Fire-unit availability
   - Crew reliability

3. Range limitations
   - Maximum and minimum effective altitude
   - Minimum effective range
   - Maximum effective range as a function of altitude
   - Maximum detection range
   - Exclusion half angle

4. Delay times and other engagement-related time intervals (stochastic)
   - Radar scan times; pop-up criterion range
   - Acquisition/time step for visual acquisition

(fixed)
  Track delay
  Intershot delay; shots/salvo
  Between engagements delay
  No warning delay
  Other time constants--breaklock, track look-ahead

5. Intercept determination
  Initial velocity
  Average deceleration
  Weapon guidance type

6. Kill determination
  Firing reliability
  Maximum SSPK as a function of altitude
  Fall-off of SSPK with range

Table B-1 depicts the ADAM Input Weapon Data Sheet which must be filled in for each participating air defense system in order to simulate its behavior in the model. Actual input data for the SA-4, SA-6, SA-7, SA-8, SA-9 and Long Track are included in Appendix A.

Each parameter will be discussed individually in terms of its utilization within the model in the remainder of this section.

B-3.2 INTERPRETATION OF WEAPON SYSTEM PARAMETERS

B-3.2.1 Initialization

Fire Units/Site: A fire unit is defined operationally as an element at a site location which can independently

Table B-1. ADAM Input Weapon Data Sheet.

IDENTIFICATION: _____

WEAPON (W,I) NAME _____ W = _____

I	DESCRIPTION	COMMENT	VALUE
1	Weapon Guidance Type		
3	Engagement Rmx		
4	Engagement Rmn		
5	Engagement Hmx		
6	Engagement Hmin		
10	Max Detection Range, Single Blip		
35	Pop-Up Criterion Range		
13	Exclusion 1/2-Angle for IR Systems (deg)		
30	Initial Velocity		
31	Average Deceleration		
33	Radar Scan Time (uncued by Long Track)		
2	Radar Scan Time (cued by Long Track)		
7	Track Delay Time		
8	Intershot Delay Time, Same Target		
34	Between Engagements Delay Time		
15	Acquisition Break-Lock Time		
37	Track Look-Ahead Time		
9	No Warning Delay		
19	Acquisition Probability/Time Step: Visual Acq.		
16	Fire Unit Availability		
36	Crew Reliability		
17	Weapon System Firing Reliability		

NH	ALTITUDE	I	Rmx(I)	I	SSPK(I)
1	38 m	20		25	
2	75 m	21		26	
3	150 m	22		27	
4	300 m	23		28	
5	7500 m	24		29	

SITE (I,K)		
8	Shots/Salvo	
13	Fire Units/Site	
27	Initial Available Number of Shots	

track and fire upon a target. The number of targets which can simultaneously and independently be tracked and fired upon by a site is the number of fire units per site. The input to the model is the original number of fire units per site. The model may diminish this number by means of the Fire Unit Availability and Crew Reliability factors.

SA-7 teams and ZSU-23-4 or SA-9 platoons, whose fire units are normally deployed in close proximity to each other, may be entered into the model as a single site with multiple fire units. The Long Track acquisition radar often appears in pairs and may be treated as a modified weapon system, incapable of firing on a target, with two "fire units" per site. Four is the current limit on fire units per site.

Initial Available Number of Shots: The Initial Number of Shots (or bursts in the case of guns) is the number of shots available to a site for all of its fire units at the beginning of a battle. The shots are shared freely among the site's fire units but are not shared between sites.

In the model, a "battle" consists of a specified number of attack waves, each flying the same profile. The user has three options regarding weapon reload. He may choose to never reload, to reload to the initial level prior to the start of each new battle, or to reload to the initial level before each attack wave.

B-3.2.2 Defense System Availability

Fire Unit Availability: At the beginning of each battle the probability that a fire unit will be operationally available for the battle (independent of the performance of

the weapon's crew) is the Fire Unit Availability. This probability is used to determine in a Monte Carlo fashion the fire units of a particular type which will be operational for the upcoming battle. If, at the beginning of a battle, N(w) is the number of fire units of type w distributed among all sites and P_F is the fire unit availability, then the expected number of viable fire units is $P_F \cdot N(w)$. The model logic forces $P_F \cdot N(w)$, rounded to the nearest integer, fire units to be available by randomly deleting fire units until $P_F \cdot N(w)$ is reached. The number of fire units at a given site may be reduced, perhaps even to zero, by this process. When no fire units remain at the site, it becomes non-operational for the battle. As long as at least one fire unit is operational at a site, all of the ammunition currently available at the site is at the disposal of the remaining fire units. Values for P_F tend to range between 0.7 and 0.9.

Crew Reliability: Crew Reliability is the probability that a fire unit which is operationally available at the beginning of a wave will indeed be available when crew-related factors are considered. This probability is used in a Monte Carlo fashion prior to each wave to determine which of the $P_F \cdot N(w)$ of the operationally available fire units of type w will be able to engage targets in the wave if the opportunity should present itself. If P_C represents the crew reliability, approximately $P_C \cdot P_F \cdot N(w)$ fire units will be available on any given wave. The actual fire units down for crew-related factors will vary from wave to wave. Those down for operational reasons will be down for the entire battle. Typical values for P_C, the crew reliability, range from 0.5 to 0.9.

B-3.2.3 Range Limitations

Intercept Envelope: The Intercept Envelope is that region where a weapon system could effectively intercept a target. For most active and semiactive command-guided missile systems, the intercept envelope is represented in ADAM as a spatial region similar to that shown in Figure B-8 below.

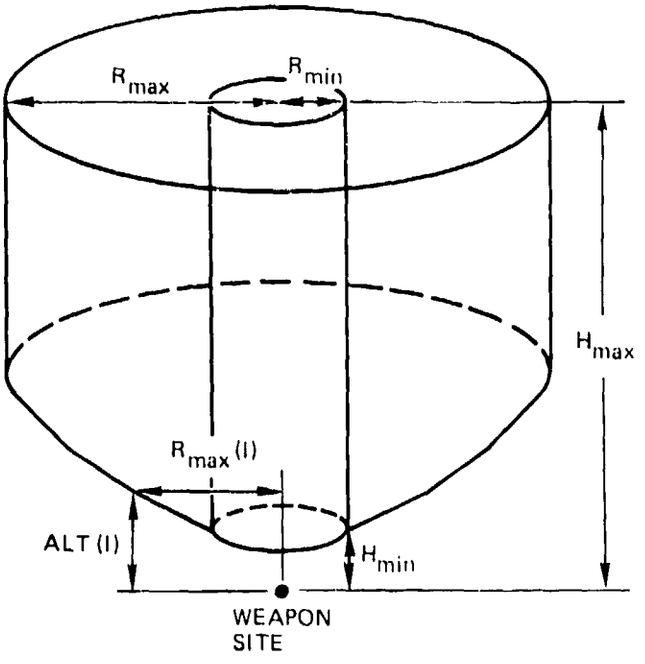

Figure B-8. Intercept Envelope for Command-Guided Missile Systems

The region is somewhat cylindrical in shape with an outer radius equal to R_{MAX}, the maximum effective range, and an inner radius equal to R_{MIN}, the minimum effective range. The upper boundary is determined by H_{MAX}, the maximum effective altitude. The lower bounding surface varies in height with the range from the site, as determined by $R_{MAX}(I)$, I = 1-5, the maximum effective range as a function

of discrete altitudes. Linear interpolation is used between specified values. The decrease in maximum range with decreasing altitude is due to the effects of the earth's surface on the radar.

The intercept envelope for gun systems is not taken as symmetrical. It resembles two half cylinders of different radii joined together and encompassing a small hollow core of radius R_{MIN}. (See Figure B-9.)

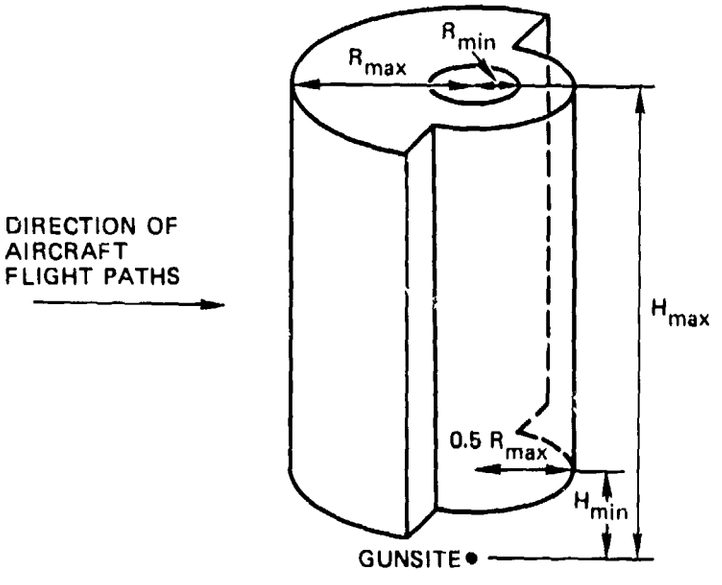

Figure B-9. Intercept Envelope for Gun System

The outer radius in the forward hemisphere is taken as R_{MAX}; the outer radius in the rear hemisphere is 0.5 R_{MAX}. Gun systems, in ADAM, thus have greater range capability in the forward hemisphere than in the rear hemisphere.

The intercept region for IR missiles resembles the region in Figure B-10 where θ is the "exclusion half angle." The forward intercept region is reduced by the exclusion half

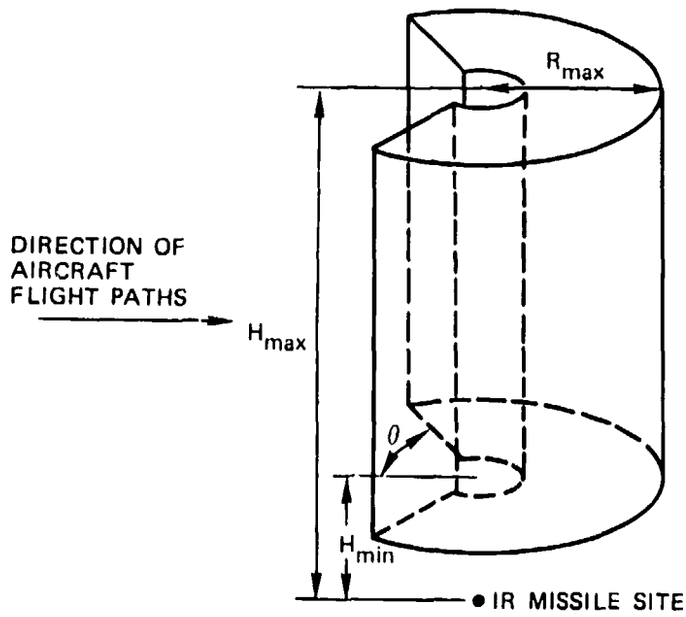

Figure B-10. Intercept Envelope for IR Missile System

angle to correspond to the IR characteristics and velocity of the target and the weapon system's capability to lock on to the different wavelengths. The intercept region is effectively reduced further in ADAM by means of the Maximum Detection Range.

A fire unit will not fire against an aircraft unless the computed intercept point falls within the intercept envelope.

Maximum Detection Range: For radar systems the Maximum Detection Range, R_{MAXDET}, is the range beyond which acquisition cannot take place. Hence, it places an outer limit upon where the first step toward a successful engagement can be taken. Other limiting factors must also be taken into

account. For IR systems, the maximum detection range was fitted to Humro data on the visual detection of aircraft.

As noted in Section B-1, there is an "engagement area" about a weapon site outside of which engagement of a target will not be attempted. It is generally more limiting than the maximum detection range taken alone and is designed to eliminate at the outset engagement sequences which are likely to result in intercept points outside the effective range of the system. In addition to the maximum detection range and maximum intercept range, determination of the engagement region involves radar scan time which has not yet been discussed. The engagement area will therefore be defined later in this section.

B-3.2.4 Delay Times - Stochastic

Although each of the delay times considered would in reality vary in length from one engagement to another, only the acquisition times are variable in the model. The variation in these times is fairly well understood. It would, on the other hand, be presumptuous to attempt to predict the probability distributions of the track delay, between engagement delay or no-warning delay, based on our limited knowledge of these times. Hence, these delays (as well as the intershot delay for which a relatively constant value would be expected) are treated as constants in the model.

Acquisition Time - Radar: Each weapon system currently used in the model, except the SA-7 and SA-9 IR systems, employs on-site radar to acquire a target. Once a target is line-of-sight visible and within detection range, three

passes by the scanning radar are considered sufficient to acquire the target. If the acquisition radar is performing a circular scan of period τ_s, the acquisition time delay will be between 2 τ_s and 3 τ_s, depending upon the radar's direction when the target first appears. The acquisition time delay used by ADAM is $(2 + RANF) \cdot \tau_s$ where RANF is a random number between zero and one. Two values of τ_s are specified for a given system. One represents uncued or autonomous operation; the other represents acquisition with the aid of Long Track cueing data. The Pop-Up Criterion Range is used in the acquisition logic to speed up the acquisition process when penetrators suddenly appear to the radar at relatively close range. When the range at which the penetrator first appears is within the pop-up range, acquisition requires two radar blips instead of three. In such cases, the acquisition time delay employed in ADAM is $(1 + RANF) \cdot \tau_s$, where RANF is a random number between zero and one.

Acquisition Time - Visible: The Acquisition Probability Per Time Step together with the maximum detection range was fitted to field-test data on the visual detection of aircraft. The numerical values obtained presumed a 1-sec time step and an aircraft speed of 230 m/sec. Thus, the corresponding distance increment was $\Delta x = 230$ m, and an on-site observer will have had $(R_{MAXDET} - x)/\Delta x$ time steps to acquire a target which has reached a distance of x meters from him and is approaching at zero offset. (R_{MAXDET} is the maximum detection range.) If p_a represents the probability of acquisition per unit time step and $P_a(x)$ is the probability that the target has been acquired by the time it is within x meters of the site, we have

$$P_a(x) = 1 - (1-p_a)^{\frac{R_{MAXDET} - x}{\Delta x}} \qquad \text{(B-5)}$$

The cumulative distribution function, $P_a(x)$, is known approximately from field tests. Values for p_a and R_{MAXDET}, as required by the model, were obtained by curve fitting techniques. The fit was reasonable (within ten percent) relative to the Humro composite data for an unaided observer out to 4.5 km. Beyond that point the fit deteriorated. Visual target acquisition is simulated in ADAM by using Monte Carlo techniques. When a target is within R_{MAXDET} and line-of-sight visible, acquisition is tested by means of a random draw against p_a. If acquisition fails, the process is repeated at succeeding time steps until the target is acquired or is out of range.

B-3.2.5 "Engagement Area"

The engagement area surrounding a site is derived from R_{MAXDET}, R_{MAX} (for the appropriate altitude) and τ_s, the radar scan time; its orientation depends on the direction from which aircraft are approaching. It is defined differently for radar-guided missile systems, IR missile systems and gun systems. A weapon site will only attempt to acquire aircraft whose x and y coordinates lie within the engagement area. The aircraft's altitude must also be between the site's minimum and maximum effective altitudes.

Radar-Guided Missile Sites: The engagement area is a rectangle containing the site. R_{MAXDET} is typically much larger than R_{MAX}, the maximum effective range. For this

case the engagement region would resemble the region shaded in Figure B-11.

IR Missile Sites: For the SA-7 and SA-9 sites, R_{MAXDET}, as entered in the model, is somewhat smaller in magnitude than R_{MAX}. For a specified exclusion half-angle θ, the region in which the engagement sequence could be initiated is shaded in Figure B-12. The effective intercept region is outlined by the dashed curve.

Gunsites: The maximum detection range for the ZSU-23-4, the only gun system simulated for the analysis in this report, far exceeds the maximum effective range. The engagement region is shaded in Figure B-13.

B-3.2.6 Delay Times - Fixed

Track Delay Time: Once a target is acquired, the time interval before the first missile (or shot) leaves the launcher is the Track Delay Time. This time is required for such purposes as establishing track, positioning the launchers, performing intercept calculations, identifying the target, establishing seeker lock-on, and making decisions. If a fire unit fires and misses and is able to reattack the same target, only the track delay time is applied before the next missile or missiles are fired at the same target.

Intershot Delay Time, Shots/Salvo: The Intershot Delay Time is the time between missile launches or gun bursts in a salvo fired at the same target. A fire unit need not repeat the acquisition and tracking sequences between shots of a salvo. The number of shots fired in a salvo is limited by the input parameter, Shots/Salvo, defined for each weapon

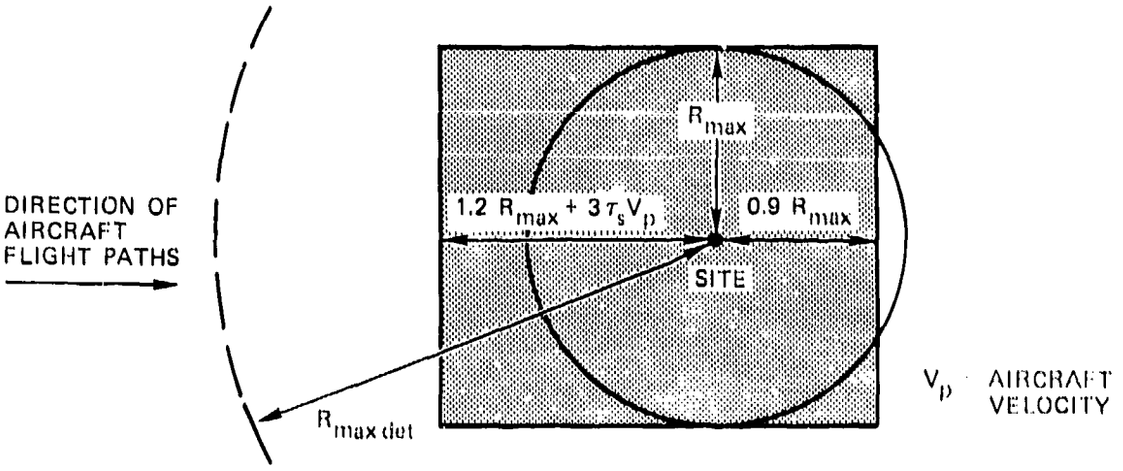

Figure B-11. Two-Dimensional Engagement Area for Radar-Guided Missile Sites

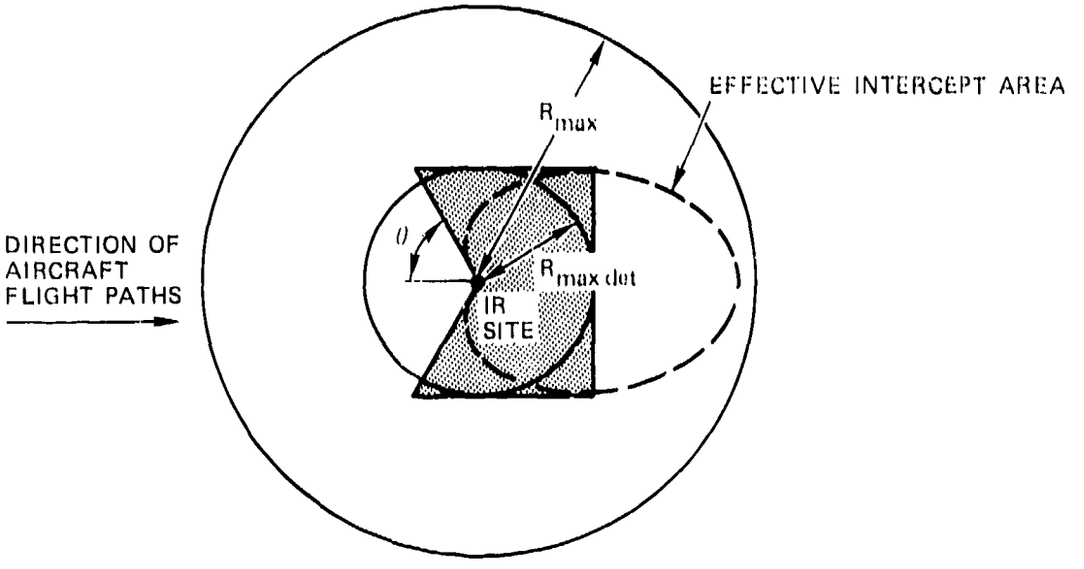

Figure B-12. Two-Dimensional Engagement Area for IR Missile Sites

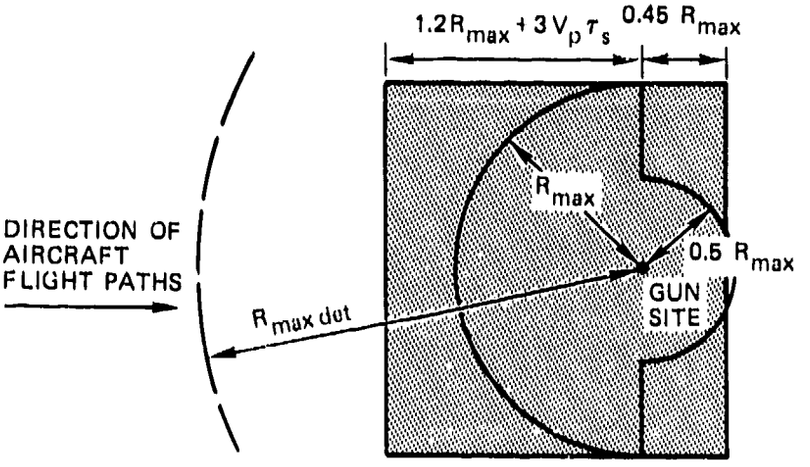

Figure B-13. Two-Dimensional Engagement Area for Gun Sites

system. This limitation could be either physical or doctrinal. The maximum value of this parameter, as allowed by the model, is six. For a gun system, no doctrinal limitation should normally be made; the maximum allowable value of six would thus be most appropriate. A weapon system will continue to fire shots at a target until its shots/salvo limit is reached or until it can no longer fire because of range, visibility or weapon availability considerations.

Between Engagements Delay Time: The time required from the time a fire unit is released from an engagement with one target until it can begin an engagement with another target is called the Between Engagements Delay Time. This delay will be followed by acquisition and track delays prior to weapon launch at the second target.

No-Warning Delay: During the first wave of a battle, a No-Warning Delay may be added to the acquisition and track delays for first engagement opportunities. After a site experiences its first engagement of the first wave or the first wave has been completed, the no-warning delay is set equal to zero. The user may elect whether or not to use the no-warning delay.

Two other times associated with a weapon system are instrumental in determining whether or not an engagement can take place. They are the Acquisition Breaklock Time and Track Look-Ahead Time.

Acquisition Breaklock Time: During the acquisition and track sequence for all systems, and during the missile fly-out period for those systems which require a line-of-sight from fire unit to target during fly-out, a break in visibility of sufficient length can nullify an engagement. The Breaklock Time is the maximum period of line-of-sight masking which the missile system can tolerate before the guidance system breaks lock.

Track Look-Ahead Time: It is presumed that either the weapon's computer or operator can project the target line-of-sight ahead for some duration (the Track Look-Ahead Time) beyond missile launch to ascertain if a breaklock situation will occur in that period. If a projected breaklock occurs within this track look-ahead time, launch will not take place. Breaklock situations farther along in the flight path will not affect missile launch and will cause command-guided or semiactive homing missiles to be counted as misses.

B-3.2.7 Intercept Point Determination

Initial Missile Velocity, Average Deceleration: Intercept point determination is a two-dimensional calculation in ADAM; aircraft altitude is neglected in the computation. For low-altitude targets, this omission is not a serious one. Furthermore, the input values of Initial Missile Velocity and Average Deceleration may be chosen so that the simulated missile's range as a function of time approximates ground range as a function of time for an actual missile fly-out profile. Appendix A, Section A-13, describes how the fly-out parameters for the study were derived from theoretical low-altitude trajectories. For high-altitude targets, initial velocity and average deceleration could be altered to fit the appropriate fly-out profile.

For the low-altitude case, the profiles of all weapon systems except gun systems were adequately approximated within the system's effective range by taking the average deceleration to be zero.

Intercept point calculations in ADAM are performed by means of one of two algorithms depending upon the type of guidance which the system is expected to use. (Both algorithms use initial missile velocity and average deceleration inputs.) The command and guidance trajectory is based on an incremental approximation to beam-rider guidance. In beam-rider guidance, the missile is maintained in the line-of-sight between weapon site and target.

The second type of guidance trajectory corresponds to proportional navigation. In proportional navigation, the

missile or gun burst proceeds along a straight line course to the projected intercept point. Proportional navigation reduces to a straight line intercept trajectory (perhaps with variable velocity) for straight-line, constant-speed targets.

Weapon Guidance Type: The type of guidance to be used, as well as the effect of aircraft nodal (turning) points on weapons in flight, is specified by means of the Weapon Guidance Type input parameter. This parameter may be assigned the value of 1, 2, 3, or 4.

Weapon Guidance Type 1 represents active command guidance. The trajectory dynamics of the missile are modeled using the approximation to beam-rider guidance. Guidance is continued through nodal points in the following sense. If the aircraft being attacked instantaneously changes position and/or direction (due to the way nodal changes occur in ADAM) while a missile is in flight, the position of the missile also undergoes an instantaneous shift in position. It is shifted so that it remains in the line-of-sight between fire unit and target and so that its distance from the target is unchanged. Due to the new direction and perhaps velocity of the aircraft, a new intercept point must be calculated.

Weapon Guidance Type 2 designates semiactive guidance. For this type of guidance, trajectory dynamics are modeled in accordance with proportional navigation. At nodal points occurring during missile flight, proportional navigation is continued. When the targeted aircraft makes a quantum jump in position at a node point, the in-flight missile is displaced by the same distance and in the same direction. In

other words, the vector displacements are identical: continuation of proportional navigation beyond the node point will yield a new intercept point.

Weapon Guidance Type 3 is intended for IR-seeking missiles. Proportional navigation is used in this case as it was for semiactive guidance. Nodal changes are handled as they were for semiactive guidance. One difference is that line-of-sight interruptions due to terrain masking occurring after missile launch will not affect or nullify the engagement. IR fire units will be released to seek other targets immediately after missile launch.

Weapon Guidance Type 4 represents radar-directed gun sites. Trajectories are based on straight-line or proportional navigation. Gun systems differ from other weapon types using proportional navigation in that shells in flight at a nodal transition cannot be reguided to a new intercept point and therefore are presumed to miss the target. Gun sites, like IR sites, are released after they fire the last burst of a salvo to seek new targets.

B-3.2.8 Kill Probability

Inputs relating directly to the effective probability of kill for an ADAM engagement are:

- $SSPK_{MAX}(I)$, I = 1-5, the maximum single shot probability of kill as a function of five discrete altitudes (38 m, 75 m, 150 m, 300 m and over 300 m). The maximum SSPK is assumed to apply to intercepts at minimum effective range.

- Weapon system firing reliability, R.

- A power, α, specifying the rate of falloff of the SSPK as a function of intercept range.

Less directly involved, but essential to the calculations, are the minimum and maximum intercept ranges, R_{MIN} and $R_{MAX}(I)$. Other inputs such as the delay times, visibility statistics, shots per salvo, and missile fly-out parameters affect the computation of kill probability by determining in a given situation where the intercept will occur, the number of shots involved and, indeed, whether an intercept is even possible.

The effective probability of kill for an engagement in process, denoted as P_K, is computed from the formula

$$P_K = R \cdot \left[1 - \prod_{i=1}^{N} (1 - SSPK_i) \right] \qquad \text{(B-6)}$$

where N = number of shots salvoed in the engagement and

$$SSPK_i = SSPK_{MAX} - SSPK_{MAX} \left(\frac{RAN_i - R_{MIN}}{R_{MAX} - R_{MIN}} \right)^{\alpha}$$

RAN_i = intercept range for i^{th} shot of the salvo

R_{MAX} and $SSPK_{MAX}$ are the maximum intercept range and single shot probability of kill for the aircraft altitude, interpolated if necessary between the appropriate discrete input values.

If the target has not previously been killed by another fire unit, a random draw against the P_K is performed at the computed intercept time. If the engaging weapon site kills the target, one shot of the salvo is presumed to kill the target while the rest of the salvo is considered wasted. If the target is not killed, all shots are classed as misses.

This logic, though reasonable for salvos of missile firings, is not meaningful for gun systems. In reality, a gun system tracks the target and fires sequential bursts of rounds in a continuous manner until the aircraft is killed or until the gun is unable to continue firing because of range, or shell supply limitations. Within ADAM, a gun continues firing until it is unable to continue because of range limitations, lack of ammunition, or the shots per salvo restriction; it does not stop when the target is killed. The composite kill probability for N bursts can be computed from Equation (B-6) where $SSPK_{MAX}$ is the single burst probability of kill corresponding to the minimum intercept range. In order to model the gun engagements better, ADAM has been modified to "determine" which burst of the salvo-sequence (if any) killed the aircraft so that subsequent bursts of the salvo can be recredited to the gun's munition supply.

From Equation (B-6), an average single-burst miss probability, Q, may be derived.

$$Q = \left[1 - \frac{P_K}{R}\right]^{1/N} \qquad \text{(B-7)}$$

The probability $P_K(k)$ that the aircraft was killed by some burst up to or including the k^{th} burst, $k \leq N$, is then

$$P_K(k) = R \cdot \left[1 - Q^k\right] \qquad \text{(B-8)}$$

A random number, RANF ($0 \leq RANF \leq 1$), is selected corresponding to $P_K(k)$. Equations (B-7) and (B-8) give a formula for the burst, k, which kills the aircraft:

$$k = \left\{ N \frac{\log\left[1 - \frac{RANF}{R}\right]}{\log\left|1 - \frac{P_K}{R}\right|} \right\}_{\substack{\text{nearest} \\ \text{integer}}} , \quad RANF \leq P_K \qquad \text{(B-9)}$$

If $RANF > P_K$, the aircraft survives all bursts of the salvo. Otherwise, the aircraft is killed on the k^{th} burst, k-1 bursts are misses, and N-k bursts are restored to the gun's supply of ammunition.

B-3.3 ACQUISITION RADARS SUCH AS LONG TRACK AS MODIFIED FIRE UNITS

Command and control may be modeled to a limited extent in ADAM by simulating the handoff capability of Long Track or other acquisition radars to netted fire units.

Acquisition radars of interest are positioned in the battlefield and treated as fire units which do not actually attack targets. The appropriate input parameters for such radars are:

Minimum intercept (acquisition) radar

Maximum intercept (acquisition) range as a function of altitude

Maximum detection range

Pop-up criterion range

Radar scan time
Acquisition breaklock time
Fire units per site

and, in some situations, fire unit availability and/or crew reliability. Each site must also be assigned a terrain-related intervisibility profile.

The acquisition process proceeds as it does for a fire unit acting autonomously. Two to three scans are required against a visible target for acquisition outside the pop-up range; one to two scans are required for targets within the pop-up criterion range. After the Long Track or other acquisition radar acquires a track, it is capable of handoff to its netted fire units so long as the target remains visible (except for intervals less than the breaklock time). A track which is under Long Track surveillance is flagged. When netted fire units attempt to engage a flagged fire unit, they apply the cued scan time for acquisition rather than their normal uncued scan time.

The cued scan time may be thought to represent a message transmission time. Its length is a measure of command and control efficiency.

SECTION B-4. SIMULATION OF DEFENSE SUPPRESSION TECHNIQUES IN ADAM

ADAM parameters can be varied to simulate various methods of air defense suppression. In the following, we discuss jamming, antiradiation missile effects and "leap frogging" of radars in response to the Precision-Emitter Location Strike System (PELSS).

B-4.1 JAMMING OF AIR DEFENSE RADARS

Different types of jamming have different effects upon a fire unit's capability to detect, track, fire upon or kill a target.

Self-screen noise jamming may be applied against either the acquisition or tracking radars but is most effectively used against the tracking radar. The mainlobe jamming thus achieved denies range information to the radar and thereby inhibits the launch of a radar-guided missile prior to burn-through unless the missile has a home-on-jam (HOJ) capability or unless optical range-finding techniques are used.

Escort jamming differs from self-screen jamming in that HOJ options may only be used against the escorts; other aircraft cannot be attacked by radar-guided missiles until radar burnthrough is achieved unless optical tracking is used.

Standoff jamming (SOJ) may be either ground-based or airborne. It has the effect of reducing the radar detection range to the burnthrough range induced by the jamming. The burnthrough range is highly dependent upon the relative geometry and characteristics of the radar, the jammer and the aircraft target.

Deception jamming can increase confusion by creating false targets prior to missile launch or may work to deceive the guidance system after launch by means of techniques such as gate stealing.

B-4.1.1 Self-Screen Noise Jamming

The jamming aircraft are detectable by the radar beyond normal radar range as long as a clear line-of-sight (LOS) exists. Most of the air defense radars are able to detect aircraft far enough away that LOS dominates R_{MAXDET} against low-altitude penetrators. Thus increasing R_{MAXDET} would have little effect. The No-Warning Delay option is not played in the presence of self-screen jamming.

Self-screen jamming denies the radar information on the aircraft range and on the number of aircraft in the vicinity of the jammer. It provides only angular information. The jamming enters the mainlobe of the tracking radar when the radar is pointed at the target. The tracking radar must achieve burnthrough before radar-guided missiles (without HOJ capability) can be launched, unless it is assisted by the optical tracker. Self-screen jamming where HOJ is not an option may be modeled in ADAM by reducing the maximum intercept range R_{MAX} to a value consistent with the calculated burnthrough range. When HOJ is an option or launch based on optical tracking is expected, the SSPK should be reduced to correspond to the increased intercept errors expected. R_{MAX} should not be reduced. Optical tracking may also result in an increased Track Delay Time.

Jamming of this sort generally increases confusion. The effects of confusion are difficult to estimate but could be played in ADAM as an increased Track Delay Time.

B-4.1.2 Escort Jamming

Escort jamming can be simulated in ADAM in a manner similar to self-screen jamming. R_{MAX} should be reduced in accordance with burnthrough range for the non-escort aircraft (and for the escort aircraft, as well, if there is no HOJ capability). The HOJ option, when present, may only be used against the escort aircraft. Since ADAM does not distinguish escort jammers from other aircraft, scenarios involving both escort jamming and HOJ missiles must be handled somewhat artificially by running the escort aircraft and other aircraft separately.

B-4.1.3 Standoff Jamming

Standoff jamming (SOJ) against the acquisition radars will affect the mainlobe of the radar when the radar is directed at a jammer and will affect the sidelobes otherwise. The burnthrough pattern that results will thus be a function of azimuth, with targets on a line with the radar and a jammer achieving the deepest penetration prior to burnthrough. It will generally be impossible for a target aircraft to take advantage of mainlobe jamming against all the air defense radars in a region.

The effect of SOJ against an acquisition radar is thus to decrease the maximum detection range, R_{MAXDET}, in an azimuth-dependent manner. ADAM, however, can accommodate only one value of R_{MAXDET} per weapon type. To determine a single representative value, the flight paths and burnthrough patterns for radars which are likely to be involved in the battle must be examined prior to running the model. This approximation is not very satisfactory, especially when there

are several jammers positioned at different azimuths or fire units of a given type at different geometries relative to the flight path and jammers. In the first case, penetrating aircraft flying by a site would in reality benefit from the effects of mainlobe jamming alternated with the effects of sidelobe jamming. In the second case, the jamming effects could vary greatly from one fire unit to another.

B-4.1.4 Deception Jamming

Deception jamming can take various forms, and its effects are generally difficult to quantify because of a lack of knowledge as to how the radars and their operators will respond. The effects of techniques that influence the missile after launch may be approximated by reducing either the weapon system's firing reliability or the probability of kill. Other techniques that serve to confuse the operator prior to launch may be simulated by increasing the Track Delay Time. In any case, the effects must be analyzed off-line and played relatively simplistically in the model.

B-4.2 ANTIRADIATION MISSILES

Radars may respond to an antiradiation missile (ARM) threat by shutting down entirely for a period of time, by shutting down until they are cued to a target by a Long Track or another acquisition radar, or by operating in a blinking mode. A radar "blinks" by alternately emitting and remaining silent at intervals designed to deter the anticipated ARM threat.

B-4.2.1 Radar Shutdown

Specific radars may be removed at the outset of the battle, or a fraction of a given type may be selected randomly and shut down on a wave-to-wave or battle-to-battle basis. The random shutdown is accomplished by means of the Availability and Crew Reliability inputs. Wild Weasel routines incorporated into ADAM serve to shut down threatened radars for a specified number of waves.

The situation where the Long Tracks remain operative and pass information to acquisition radars which otherwise are silent can be simulated by assigning very large numbers to the uncued scan times of the weapon systems involved. The weapon systems can then acquire only when the target is visible to and has been acquired by an associated Long Track. The handoff time from the Long Track to the fire control radar can be varied by means of the cued scan-time.

B-4.2.2 Radar Blinking

The influence of radar blinking on the effectiveness of an acquisition radar can be modeled in ADAM by increasing the radar's uncued scan period, τ_s. If ϕ is the fraction of time that the radar emits, then the effective scan period is $\tau_s' = \tau_s/\phi$.

Blinking could be effective against ARMs but would not protect an air defense site from being located by Wild Weasel or a PELSS-type system or from being attacked by PGMs or other munitions delivered to the target location.

B-4.3 LOCATOR/DESTRUCTION SYSTEMS (e.g., PELSS)

If a standoff (airborne or surface deployed) locator destruction system has been deployed and the air defenders are aware of its existence, the defenders might elect a simple emit-move-emit (EME) counter to such a system. A possible model for an EME strategy would be (1) where only the pertinent radar antenna would be moved and only over relatively short distances or (2) where possibly two radars would be cycled cooperatively for the same set of TELs.

The fractional emission efficiency, f_E, for this strategy is defined as the fraction of time that some radar associated with the fire units is operating. This is given by

$$f_E = \frac{N \cdot T_{ED}}{T_{ED} + T_K}$$

where T_K = knockdown/move/set-up time for the antenna
N = number of cooperating radars (per fire unit)
T_{ED} = emission dwell time

In this model, T_{ED} is a variable which the defender would adjust to attain a desired degree of survivability while maximizing the operational readiness of the defenses. The strategy would be modeled in ADAM by equating the fractional emission efficiency, f_E, to the Fire Unit Availability or the Crew Reliability or a suitable combination of the two. If the EME cycle can generally take place within the time frame of a single wave, the Crew Reliability factor should be used. If it takes place in the time frame of a single battle, the Fire Unit Availability would be most appropriate. In addition to the downtime due to EME, the system and

crew reliabilities would certainly be further degraded because of increased maintenance and fatigue.

Fire units might cease to emit and rely on Long Track cueing, unless or until Long Track itself was attacked. Visual acquisition is another possibility but is very difficult without accurate cueing.

B-4.4 MISCELLANEOUS DEFENSE SUPPRESSION TECHNIQUES

Several defense suppression measures not yet discussed may be simulated to some extent with ADAM. These measures are described in the following subsections.

B-4.4.1 Decoys

Decoys may be played by increasing the number of aircraft per wave and proportioning the kills among the real aircraft and the decoys.

B-4.4.2 Infrared Countermeasures and Jinking

Effects from infrared countermeasures and jinking are played by reducing the SSPK of the weapons. Also the average aircraft velocity should be reduced on legs where jinking is prevalent.

B-4.4.3 Direct Attack with PGMs

Direct attacks against fire units may be played using ADAM's Wild Weasel routines. Alternatively, the location of targets to be attacked can be noted, and flight profiles designed to attack those targets can be run. Unless precise

target locations are known prior to the mission (i.e., a system such as PELSS is operable), the attackers will have to pop-up to locate their target as well as pop-up to attack it. The success of the attack can be calculated by noting where along the path, if anywhere, the individual attackers are killed and by estimating the probability of a successful attack by surviving aircraft. The air defenses killed may be eliminated for successive waves of aircraft.

B-4.4.4 Chaff

Chaff cannot be effectively played in ADAM at present except to hypothesize the chaff location and eliminate those portions of flight paths which would be within the chaff cloud or corridor, at least when running against weapon systems susceptible to chaff.

DISTRIBUTION LIST

DEPARTMENT OF DEFENSE

Armed Forces Radiobiology Rsch Institute
Defense Nuclear Agency
ATTN: Director

Armed Forces Staff College
ATTN: Reference & Tech Svcs Br

Assistant Secretary of Defense
International Security Affairs
ATTN: Reg Dir (European)
ATTN: Policy Plans & NSC Affairs
ATTN: F. Miller
ATTN: ISA/PP

Assistant Secretary of Defense
Program Analysis & Evaluation
ATTN: S. Sienkiewiez
ATTN: Strategic Programs

Assistant to the Secretary of Defense
Atomic Energy
ATTN: Strategy & Assessment
ATTN: T. Sisson
ATTN: L. Michael
ATTN: Nuclear Policy Planning

Command & Control Tech Ctr
ATTN: C-312, R. Mason

Commander-in-Chief, Pacific
ATTN: C3SRD

Defense Intelligence Agency
ATTN: Lib
ATTN: DB-4C, E. O'Farrell
ATTN: DN
ATTN: DB-4C, P. Johnson
ATTN: RTS-2C
ATTN: DIO-GPF, W. Magathan
ATTN: DT-J, Vorona

Defense Nuclear Agency
ATTN: NATA
ATTN: RAAE
ATTN: STSP
ATTN: SPTD
ATTN: STNA
ATTN: STRA
ATTN: NASD
ATTN: RAEE
ATTN: NATD
ATTN: NAFD
4 cy ATTN: TITL

Defense Tech Info Ctr
12 cy ATTN: DD

Field Command
Defense Nuclear Agency
2 cy ATTN: FCP, J. T. McDaniel

Field Command
Defense Nuclear Agency
Livermore Branch
ATTN: FCPRL

DEPARTMENT OF DEFENSE (Continued)

Field Command
Defense Nuclear Agency
ATTN: FCPRA

Interservice Nuclear Weapons School
ATTN: Document Control

Joint Chiefs of Staff
ATTN: J-5 Nuclear/Chemical Policy Br, J. Steckler
ATTN: SAGA/SFD
ATTN: J-5 Strategy Div, W. McClain
ATTN: J-3
ATTN: J-5 Nuclear Div/Strategy Div
ATTN: SAGA/SSD

Joint Strat Tgt Planning Staff
ATTN: JP
ATTN: JPPF
ATTN: JLTW
ATTN: JL

National Defense University
ATTN: NWCLB-CR

Director
Net Assessment
Office of the Secretary of Defense
ATTN: F. Giessler
ATTN: Military Assistants
ATTN: LTC Bankson

US European Command
ATTN: J-3
ATTN: J-5

US National Military Representative
SHAPE
ATTN: US Doc Ofc for Intel
ATTN: US Doc Ofc for PANDP
ATTN: US Doc Ofc for OPS (Nuc Plans)

Under Secretary of Defense for Policy Plng
ATTN: Dir Strategic Policy, C. Estes
ATTN: Dir Plng & Requirements, M. Sheridan
ATTN: Dir Negotiations Policy, S. Buckley

Under Secretary of Defense for Rsch & Engrg
ATTN: Strategic & Space Sys (OS)
ATTN: M. Minneman
ATTN: F. McLesky
ATTN: K. Hinman

DEPARTMENT OF THE ARMY

Deputy Chief of Staff for Ops & Plans
Department of the Army
ATTN: DAMO-RQA
ATTN: DAMO-RQS
ATTN: DAMO-SSM
ATTN: DAMO-NCN
ATTN: DAMO-SSP, COL Sewall
ATTN: Tech Advisor

DEPARTMENT OF THE ARMY (Continued)

Deputy Chief of Staff for Rsch Dev & Acq
ATTN: DAMA-CSM-N

Eighth US Army
ATTN: CJ-JP-NS

Asst Chief of Staff for Intelligence
ATTN: DAMA-RT
ATTN: Div of Foreign Intelligence

Harry Diamond Laboratories
Department of the Army
ATTN: DELHD-N-TD
ATTN: DELHD-N-D
ATTN: 00100, Commander/Tech Dir/TSO
ATTN: DELHD-N-P
ATTN: Chairman Nuc Vulnerability Br

US Army Armament Rsch Dev & Cmd
ATTN: DRDAR-LCN-E

US Army Armor School
ATTN: ATSB-CTD

US Army Ballistic Rsch Labs
ATTN: DRDAR-TSE-S
ATTN: DRDAR-VL
ATTN: DRDAR-BLV

US Army Air Defense School
ATTN: COL Rinehart

US Army Comd & General Staff College
ATTN: Combined Arms Rsch Lib

US Army Concepts Analysis Agency
ATTN: CSSA-ADL

Commander-in-Chief
US Army, Europe and Seventh Army
ATTN: DCSI-AEAGB-PDN
ATTN: AEAGC-O-W
ATTN: J-5
ATTN: AEAGE
ATTN: O-N
ATTN: AEAGD-MM

US Army Fa Msl Sys Eval Gp
ATTN: ATZK-MG
ATTN: K. McDonald

US Army Forces Command
ATTN: AF-OPTS
ATTN: LTC Strumm

US Army Foreign Science & Tech Ctr
ATTN: DRXST-SD-1

US Army Infantry School
ATTN: ATSH-CTD

US Army Intel Threat Analysis Detachment
ATTN: IAX-ADT

US Army Intelligence Ctr & School
ATTN: ATSI-CD-CS

US Army Materiel Dev & Readiness Cmd
ATTN: DRCDE-D

DEPARTMENT OF THE ARMY (Continued)

US Army Missile Command
ATTN: DRSMI-YDR
ATTN: DRCPM-PE, W. Jann
ATTN: DRDMI-EAA, E. Harwell

US Army Mobility Equip R&D Cmd
ATTN: DRDME-WC, Tech Lib (Vault)
ATTN: DRDME-RT, K. Oscar

US Army Nuclear & Chemical Agency
ATTN: Lib
ATTN: MONA-ZB, D. Panzer

US Army TRADOC Sys Analysis Actvy
ATTN: ATAA-TAC

US Army Training and Doctrine Comd
ATTN: ATCD-D, COL Kravciez
ATTN: ATCD-CF

US Army War College
ATTN: Lib

V Corps
Department of the Army
ATTN: Commander
ATTN: G-3

VII Corps
Department of the Army
ATTN: Commander

DEPARTMENT OF THE NAVY

Anti-Submarine Warfare Sys Proj Ofc
Department of the Navy
ATTN: PM-4

Charleston Naval Shipyard
ATTN: Commanding Officer

Crusier Destroyer Group One
Department of the Navy
ATTN: N321

David Taylor Naval Ship R&D Ctr
ATTN: Code 142-3
ATTN: Code 1750, W. Conley
ATTN: Code 174
ATTN: 1750, J. Sykes

Joint Cruise Missiles Project Ofc
Department of the Navy
ATTN: JCMG-707

Marine Corps
Department of the Navy
ATTN: DCS (P&O), Strategic Plans Div
ATTN: DCS (P&O) Requirements Div
ATTN: Code OIOC-31

Marine Corps Dev & Education Command
Department of the Navy
ATTN: Commander

Naval Air Development Ctr
ATTN: Code 702, B. McHugh

Naval Air Systems Command
ATTN: Code 350D, H. Benefiel

DEPARTMENT OF THE NAVY (Continued)

Naval Intelligence Command
ATTN: NIC-01

Naval Intelligence Support Ctr
ATTN: NISC-30
ATTN: NISC-40

Naval Material Command
ATTN: MAT-00
ATTN: MAT-046

Naval Ocean Systems Ctr
ATTN: J. Hooper
ATTN: R. Hammond

Naval Postgraduate School
ATTN: Code 1424, Lib
ATTN: Code 56PR

Naval Rsch Lab
ATTN: Code 2627

Naval Sea Systems Command
ATTN: SEA-06H2
ATTN: SEA-406
2 cy ATTN: SEA-6431G, H. Sequine

Naval Submarine Base
ATTN: Commanding Officer

Naval Submarine School
ATTN: Commanding Officer

Naval Surface Force, Atlantic
ATTN: Commander

Naval Surface Force, Pacific
ATTN: Commander

Naval Surface Weapons Ctr
ATTN: Code 130
ATTN: Code 041
ATTN: Code 131
ATTN: Code 012
ATTN: Code R14

Naval Surface Weapons Ctr
ATTN: Code DG-502, L. Freiling

Naval War College
ATTN: Code E-11 (Tech Service)

Naval Weapons Ctr
ATTN: Code 32607, L. Thompson

Naval Weapons Evaluation Facility
ATTN: Tech Dir
ATTN: G. Binns

Navy Field Operational Intelligence Off
ATTN: Commanding Officer

Newport Laboratory
Naval Underwater Systems Ctr
ATTN: K. Walsh

Nuclear Weapons Trng Group, Pacific
Department of the Navy
ATTN: Nuclear Warfare Department

DEPARTMENT OF THE NAVY (Continued)

Nuclear Weapons Trng Group, Atlantic
Department of the Navy
ATTN: Nuclear Warfare Department

Office of Naval Rsch
ATTN: Code 431
ATTN: Code 200

Office of the Chief of Naval Operations
ATTN: OP 953
ATTN: OP 954
ATTN: OP 098
ATTN: OP 00X
ATTN: OP 32
ATTN: OP 35
ATTN: OP 50
ATTN: OP 963
ATTN: OP 950
ATTN: OP 951
ATTN: OP 985F
ATTN: OP 654
ATTN: OP 09
ATTN: OP 05
ATTN: OP 653
ATTN: OP 955
ATTN: OP 02
ATTN: OP 981
ATTN: Op 021
ATTN: OP 03
ATTN: OP 987
ATTN: OP 06
ATTN: OP 022
3 cy ATTN: OP 96
3 cy ATTN: OP 65

Office of the Chief of Naval Operations
ATTN: OP-00K

Sixth Fleet
Department of the Navy
ATTN: Commander

Surface Warfare Development Group
Naval Amphibious Base
ATTN: Commander

Surface Warfare Officers School Cmd
Department of the Navy
ATTN: Combat Systems Dept

Commander-in-Chief
US Atlantic Fleet
Department of the Navy
ATTN: Code J-5
ATTN: Code N-3
3 cy ATTN: Code N-2

US Naval Air Forces
Pacific Fleet
ATTN: Commander

US Naval Air Forces
Atlantic Fleet
ATTN: Commander

Commander-in-Chief
US Naval Forces, Europe
ATTN: R&D

DEPARTMENT OF THE NAVY (Continued)

US Navy, Second Fleet
ATTN: Commander
4 cy ATTN: ACOS TAC D&E Div

US Navy, Seventh Fleet
ATTN: Commander

US Navy, Third Fleet
ATTN: Commander

Commander-in-Chief
US Naval Forces, Europe
US Pacific Fleet
ATTN: CINC
ATTN: Code N2

US Submarine Force
Department of the Navy
Atlantic Fleet
ATTN: Commander

US Submarine Force
Department of the Navy
Pacific Fleet
ATTN: Commander

DEPARTMENT OF THE AIR FORCE

Air Force Academy
ATTN: Lib

Air Force Test & Evaluation Ctr
ATTN: OA

Air Force Weapons Laboratory
Air Force Systems Command
ATTN: NSSB
ATTN: SUL

Assistant Chief of Staff
Intelligence
Department of the Air Force
ATTN: INE

Assistant Chief of Staff
Studies & Analyses
Department of the Air Force
ATTN: AF/SAG, H. Zwemer
ATTN: AF/SAMI
ATTN: AF/SAGF

Ballistic Missile Office
Air Force Systems Command
ATTN: SYE, R. Landers

Deputy Chief of Staff
Operations Plans and Readiness
Department of the Air Force
ATTN: Director of Plans
ATTN: AFXOOR
ATTN: AFXOOTR
ATTN: AFXOXFM
ATTN: AFXOXFT
ATTN: Dir of Operations & Plans

Deputy Chief of Staff
Research, Development, & Acq
Department of the Air Force
ATTN: AFRDQI
ATTN: AFRDQR

DEPARTMENT OF THE AIR FORCE (Continued)

Rapid Deployment Joint Task Force
Department of the Air Force
ATTN: RDJE-03, S. Fleming

Tactical Air Command
Department of the Air Force
ATTN: TAC/DO

Tactical Air Command
Department of the Air Force
ATTN: TAC/DR

Tactical Air Command
Department of the Air Force
ATTN: TAC/INO

Tactical Air Command
Department of the Air Force
ATTN: TAC/SMO-G

Tactical Air Command
Department of the Air Force
ATTN: Tactical Air Command/XP

Tactical Air Command
Department of the Air Force
ATTN: TAC-XPB

Commander-in-Chief
US Air Forces in Europe
ATTN: USAFE/DO&I

Commander-in-Chief
US Air Forces in Europe
ATTN: USAFE/DOA

Commander-in-Chief
US Air Forces in Europe
ATTN: USAFE/DOJ

Commander-in-Chief
US Air Forces in Europe
ATTN: USAFE/IN

Commander-in-Chief
US Air Forces in Europe
ATTN: USAFE/XPX

Commander-in-Chief
US Readiness Command
Department of the Air Force
ATTN: J-3

USAF School of Aerospace Medicine
ATTN: Radiation Sciences Div

OTHER GOVERNMENT AGENCIES

Central Intelligence Agency
ATTN: OSWR/NED
ATTN: OSR/SE/I

Federal Emergency Management Agency
National Sec Ofc Mitigation & Rsch
ATTN: Deputy Dir, J. Nocita
ATTN: Asst Dir for Rsch, J. Buchanon
ATTN: Assistant Associated Dir

US Arms Control & Disarmament Agency
ATTN, C. Thom
ATTN: A. Leiberman

DEPARTMENT OF ENERGY CONTRACTORS

Lawrence Livermore National Lab
ATTN: L-21, M. Gustavson
ATTN: L-8, F. Barrish
ATTN: L-9, R. Barker
ATTN: L-35, J. Immele

Los Alamos National Lab
ATTN: E. Chapin
ATTN: R. Stolpe
ATTN: M/S634, T. Dowler
ATTN: R. Sandoval

Sandia National Laboratories
Livermore Lab
ATTN: T. Gold

Sandia National Lab
ATTN: 3141
ATTN: 5612, J. W. Keizur

DEPARTMENT OF DEFENSE CONTRACTORS

Academy for Interscience Methodology
ATTN: N. Pointer

Analytical Technology Applications Corp
ATTN: J. Scharfen

Atmospheric Science Assoc
ATTN: H. Normeat

BDM Corp
ATTN: P. White
ATTN: J. Morgan
ATTN: H. Portnoy
ATTN: R. Buchanan
ATTN: J. Herzog
ATTN: C. Wasaff
ATTN: J. Bode
ATTN: J. Braddock
ATTN: R. Welander

Boeing Co
ATTN: L. Harding

66th MI Group
ATTN: T. Greene

Decision-Science Applications, Inc
ATTN: Dr Pugh

General Research Corp
ATTN: H. Schroeder
ATTN: Tactical Warfare Operations
ATTN: P. Lowry
ATTN: A. Berry

Hudson Institute, Inc
ATTN: H. Kahn
ATTN: C. Gray

Institute for Defense Analyses
ATTN: M. Sher

JAYCOR
ATTN: E. Almquist

DEPARTMENT OF DEFENSE CONTRACTORS (Continued)

Kaman Sciences Corp
ATTN: V. Cox
ATTN: F. Shelton

Kaman Sciences Corp
ATTN: T. Long

Kaman Tempo
ATTN: DASIAC

Kaman Tempo
ATTN: DASIAC

Mantech International Corp
ATTN: President

Martin Marietta Corp
ATTN: F. Marion
ATTN: M. Yeager

McDonnell Douglas Corp
ATTN: Tech Lib Svcs

McLean Research Ctr, Inc
ATTN: W. Schilling

McMillan Science Associates, Inc
ATTN: W. McMillan

Mission Rsch Corp
ATTN: Tech Lib

Pacific-Sierra Rsch Corp
ATTN: G. Lang
ATTN: H. Brode

Pacific-Sierra Rsch Corp
ATTN: G. Moe

R & D Associates
ATTN: A. Lynn
ATTN: R. Montgomery
ATTN: P. Haas
4 cy ATTN: H. Shoemaker

R & D Associates
ATTN: J. Bengston
ATTN: J. Thompson
ATTN: W. Houser

Rand Corp
ATTN: J. Digby
ATTN: Lib
ATTN: T. Parker

Raytheon Co
ATTN: W. Britton

University of Rochester
ATTN: NAVWAG

Santa Fe Corp
ATTN: D. Paolucci

Science Applications, Inc
ATTN: D. Kaul

DEPARTMENT OF DEFENSE CONTRACTORS (Continued)

Science Applications, Inc
ATTN: M. Drake
ATTN: C. Whittenbury
ATTN: J. Martin

Science Applications, Inc
ATTN: J. McGahan
ATTN: J. Goldstein
ATTN: W. Layson

SRI International
ATTN: J. Naar
ATTN: W. Jaye
ATTN: G. Abrahamson
ATTN: B. Gasten

System Planning & Analysis, Inc
ATTN: P. Lantz

DEPARTMENT OF DEFENSE CONTRACTORS (Continued)

System Planning Corp
ATTN: G. Parks
ATTN: I. Adelman
ATTN: J. Douglas

T. N. Dupuy Associates, Inc
ATTN: T. Dupuy

TRW Defense & Space Sys Group
ATTN: R. Anspach

Vector Research, Inc
ATTN: S. Bonder